Journal of Inclusion Phenomena and Macrocyclic Chemistry **34:** 361–391, 1999.

Review Article

Helicates and Related Metallosupramolecular Assemblies: Toward Structurally Controlled and Functional Devices

CLAUDE PIGUET*
Department of Inorganic, Analytical and Applied Chemistry, University of Geneva, 30, quai Ernest Ansermet, CH-1211 Genève 4
Tel.: (022) 702 60 34; Fax: (022) 702 68 30; E-mail: Claude.Piguet@chiam.unige.ch

(Received: 13 October 1998; in final form: 10 November 1998)

Key words: helicate, supramolecular, self-assembly, device, catenate, cage, cluster.

1. Basic Principles and Recent Advances in Helicate Self-Assembly

According to the first use of the word 'helicate' in 1987 [1] and its accepted definition [2]: a helicate is a discrete helical supramolecular complex constituted by one or more covalent organic strands wrapped about and coordinated to a series of ions defining the helical axis. The ligand strands are made of several domains corresponding to binding units coordinated to the central ions (in general cations) separated by spacers exhibiting specific structural requirements (Figure 1).

Three peculiar characteristics are associated with idealized helicates: (i) several metal ions are located on a straight line according to a mono-dimensional arrangement, (ii) the wrapped ligand strands induce helicity, a special case of chirality [3] and (iii) the final helicate is generated by a strict self-assembly process [4], i.e. it corresponds to the thermodynamically most stable complex. This latter point requires that the interactions between the strands and the metal ions are reversible in order to allow a complete exploration of the energy hypersurface of the assembly process [2, 5]. The coordinate bonds involved between the components in the helicates (i.e. the ligand strands and 3d- or 4f-block ions) are particularly well-suited for this purpose since they are labile enough to ensure reversibility, but strong enough to provide thermodynamically stable complexes. The generation of one particular supramolecular helicate thus results from the combination of two crucial factors: (1) a judicious match between the *intrinsic information* borne by the metal

* Author for correspondence.

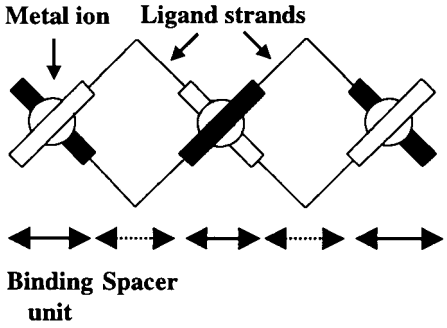

Figure 1. Schematic representation of a trimetallic double-stranded helicate.

ions (size, charge, polarizability, ligand field) and the ligand strands (denticity of the binding units, steric constraints, nature of the spacer, nature of the donor atoms) and (2) a suitable set of external constraints termed the *conditional information* which affect the thermodynamic equilibria (solvent, stoichiometry, concentration, temperature, pressure, etc. . . .). The synthetic introduction of specific intrinsic informations into the ligand strands in order to program the final helical structure has been extensively investigated during the last decade and was recently reviewed in great detail up to the beginning of 1997 [2, 6, 7]. The combination of hundreds of ligand strands and metal ions can be classified according to a simple method summarized in Figure 2 [2]. Each helicate is completely characterized by a set of four successive terms: (1) the number of strands: single-, double-, triple- or quadruple-stranded; (2) the nature of the strands: homotopic = similar binding units, heterotopic = different binding units; (3) the relative orientation of the strands in the helicate: *H* = head-to-head, *T* = head-to-tail and (4) the coordination of ancilliary ligands to the metal ions: no extra ligand = saturated, one or more ancilliary ligands = unsaturated.

For instance the sterically constrained strand **1** (Figure 3) reacts with octahedral Co(II) to give exclusively the saturated homodimetallic triple-stranded homotopic helicate $[Co_2(\mathbf{1})_3]^{4+}$ [8], while a saturated heterodimetallic double-stranded heterotopic head-to-head helicate (HH)-$[FeAg(\mathbf{2})_2]^{3+}$ is observed upon reaction of the segmental ligand **2** with tetrathedral Ag(I) and octahedral Fe(II) [9].

The search for new symmetrical segmental ligands leading to programmed helicates is still active and the oligomultidentate strands **3**–**8** lead to the expected homotopic double-stranded helicates with spherical metal ions $[Cu_2(\mathbf{3})_2]^{2+}$ [10], $[Cu_3(\mathbf{4})_2]^{3+}$ [11], $[Cu_2(\mathbf{5})_2]^{2+}$ and $[Cu_2(\mathbf{6})_2]^{2+}$ [12], $[Cd_2(\mathbf{7})_2]$ [13], $[K_2(\mathbf{8})_2]$ and $[Cu_2(\mathbf{8})_2]^{2+}$ [14]. Related homotopic triple-stranded helicates $[Ni_2(\mathbf{9})_3]^{4+}$ [15] and $[Mn_2(\mathbf{10}\text{-}2H)_3]$ [16] are obtained with octahedral metal ions. According to this reasoning, quadruple-stranded helicates have been obtained recently by the assembly of oligo-monodentate ligands **11** (penta-monodentate) and **12** (tris-monodentate) with tetragonal metal ions. In both cases $[Co_5(\mathbf{11})_4(SCN)_2]$ [17]

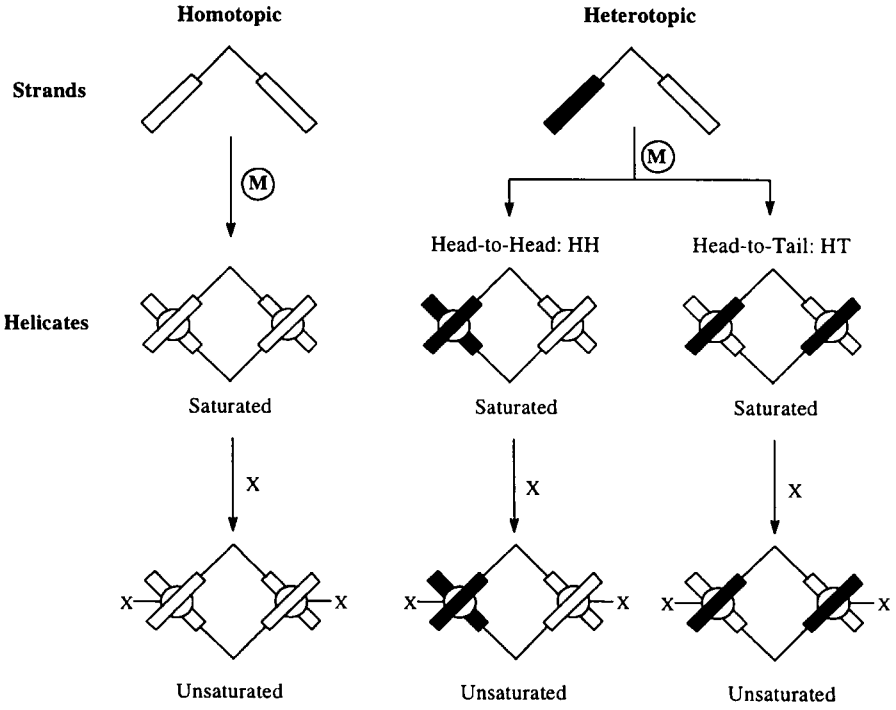

Figure 2. A classification of helicates according to the intrinsic information [2]. (Reproduced with the permission from Ref. [2]. Copyright 1997 American Chemical Society.)

and $[Co_3(\mathbf{12})_4(BF_4)_2]$ [18], the short intermetallic distances imply Co—Co bonds leading to pseudo-octahedral environments around the metal ions.

Subtle structural control may result from intramolecular interstrand interactions in the final helicate which force the generation of one particular structure. The unsymmetrically substituted quaterpyridine **13** allows the investigation of interstrand steric constraints on the orientation of the strands in the final double-stranded heterotopic helicate $[Cu_2(\mathbf{13})_2]^{2+}$ [19]. The ratio of head-to-head (HH) vs head-to-tail (HT) isomers strongly depend on (i) the bulkiness of the connected R substituents and (ii) the helical pitch (Figure 4), but steric repulsions systematically induce a pronounced preference for the head-to-head isomer.

The orientation of unsymmetrical strands may also result from the introduction of slightly different binding units along the strand. **14** possesses two similar, but not identical, bidentate binding units and reaction with Ti(IV), Ga(III) or a mixture of both metal ions in basic media produce selectively one single diastereomeric triple-stranded side-by-side complex (= 'meso helicate') [20]. Surprisingly, the head-to-tail homodimetallic isomers (HHT)-$[Ga_2(\mathbf{14}\text{-}3H)_3]^{3-}$ and (HHT)-$[Ti_2(\mathbf{14}\text{-}3H)_3]^{-}$ are quantitatively obtained in solution while the head-to-head arrangement (HHH)-$[GaTi(\mathbf{14}\text{-}3H)_3]^{2-}$ is observed for the heterodimetallic complex [20]. As an intricate mixture of eight complexes might be expected for

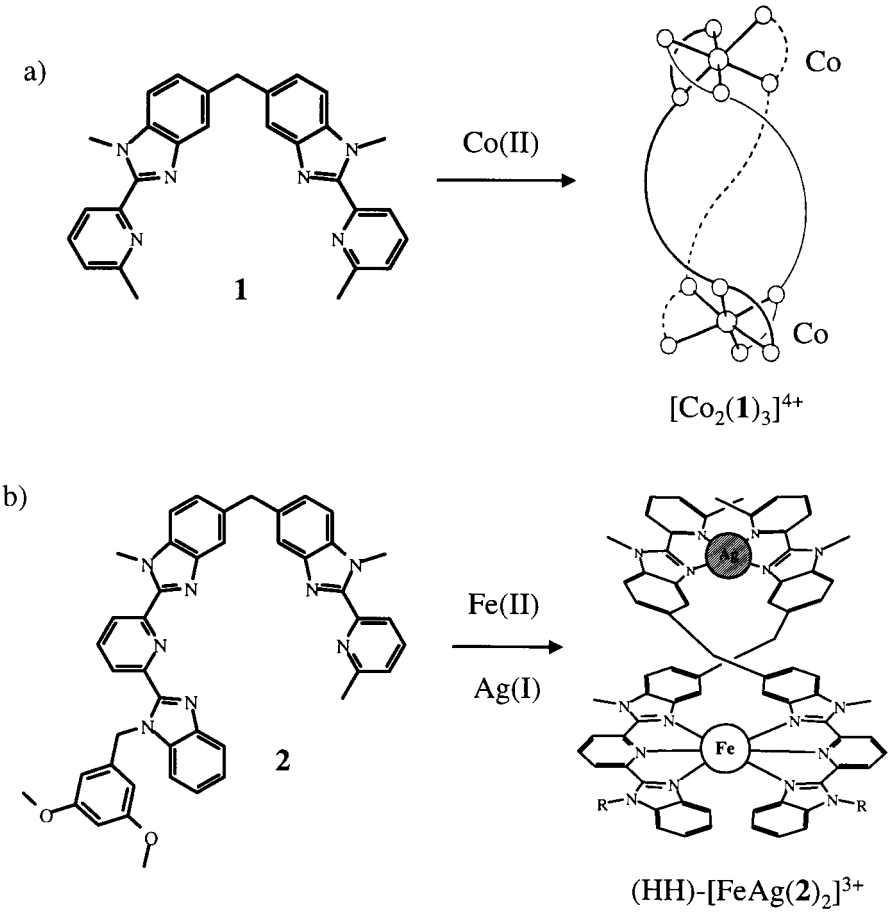

Figure 3. Self assembly of (a) the saturated homodimetallic triple-stranded homotopic helicate $[Co_2(\mathbf{1})_3]^{4+}$ [8] and (b) the saturated heterodimetallic double-stranded head-to-head heterotopic helicate (HH)-$[FeAg(\mathbf{2})_2]^{3+}$ [9].

the latter reaction: four heterodimetallic complexes ((HHH)-$[GaTi(\mathbf{14}\text{-}3H)_3]^{2-}$, (HHH)-$[TiGa(\mathbf{14}\text{-}3H)_3]^{2-}$, (HHT)-$[GaTi(\mathbf{14}\text{-}3H)_3]^{2-}$, (HHT)-$[TiGa(\mathbf{14}\text{-}3H)_3]^{2-}$) and four homodimetallic complexes ((HHH)-$[Ga_2(\mathbf{14}\text{-}3H)_3]^{3-}$, (HHT)-$[Ga_2(\mathbf{14}\text{-}3H)_3]^{3-}$, (HHH)-$[Ti_2(\mathbf{14}\text{-}3H)_3]^{-}$ and (HHT)-$[Ti_2(\mathbf{14}\text{-}3H)_3]$); the generation of a single species in solution demonstrates the crucial influence of thermodynamic equilibria which are responsible for the 'miraculous' selectivity associated with self-assembly processes. Although the factors controlling the thermodynamic equilibria in self-assembly (i.e. the conditional information) are as important as intrinsic information encoded in the components for controlling the structure of the final helicate, only few assembly processes have been fully characterized [9, 21] and the reasons for the generation of one particular complex is poorly understood. Figure 5 reports one of the few complete studies of thermodynamic equilibria involved in the

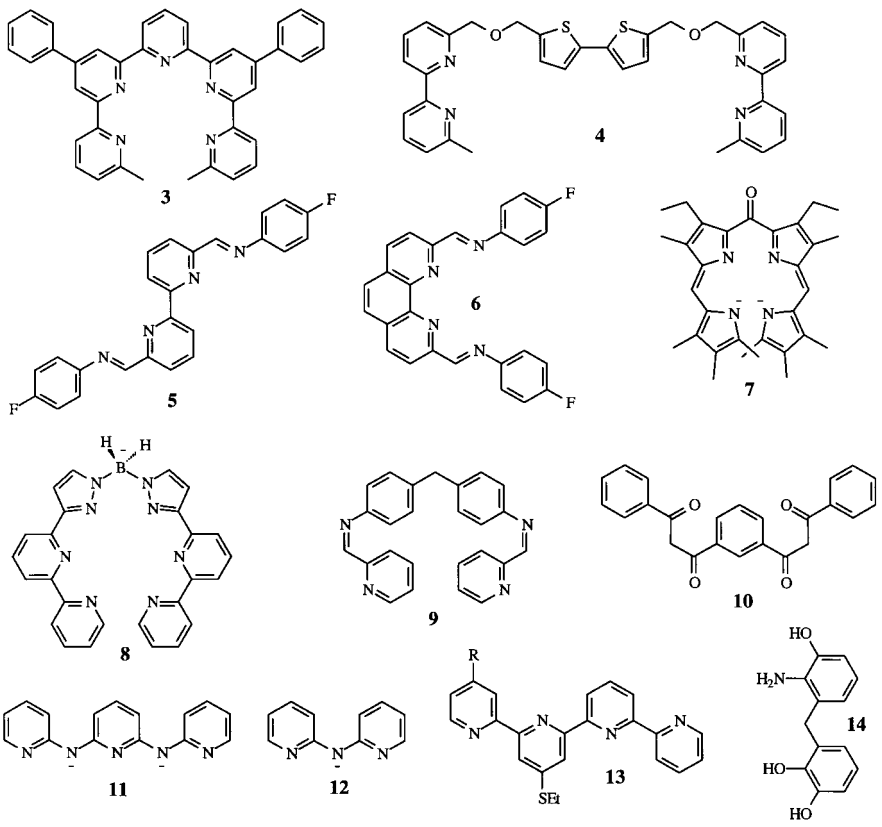

Chart 1.

formation of the self-assembled heterodimetallic double-stranded helicate (HH)-$[FeAg(\mathbf{2})_2]^{3+}$ [9]. The consideration of the stability constants predicts that the desired helicate (HH)-$[FeAg(\mathbf{2})_2]^{3+}$ is quantitatively formed (>95% of the ligand speciation) only for a precise set of conditions: a stoichiometric ratio of Fe : Ag : **2** = 1 : 1 : 3 and a total ligand concentration larger than 0.02 M. For a smaller ligand concentration, but in the same stoichiometric conditions, the heterodimetallic helicate coexists in solution with homometallic complexes under thermodynamic equilibria. Other specific sets of conditional information can be applied to select quantitatively any of the complexes involved in these equilibria. Such complicated thermodynamic processes have been recently termed 'virtual combinatorial library' by Lehn and coworkers [22], but it is rather frustrating that only few complete and reliable thermodynamic data are available for predicting helicate self-assembly with d-block [8, 9, 12, 21, 23] and f-block metal ions [24–26].

Positive cooperativity [27] is one of the recurrent characteristic which is systematically invoked to justify selectivity and completion of helicate self-assembly processes, but it has been only unambigously demonstrated by Lehn and coworkers for double-stranded helicates with Cu(I) and Ag(I) [21]. Recent investiga-

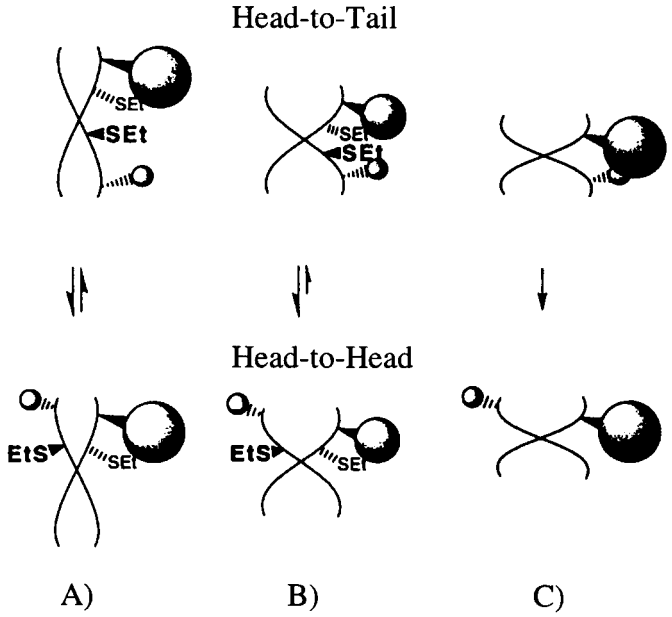

Figure 4. Interstrand interactions between substituents in $[Cu_2(\mathbf{13})_2]^{2+}$: (A) extended helicate with weakly interacting substituents; (B) intermediate helicate with medium interaction and (C) compact helicate with strongly interacting substituents [19]. (Reproduced with the permission from Ref. [19]. Copyright 1997 American Chemical Society.)

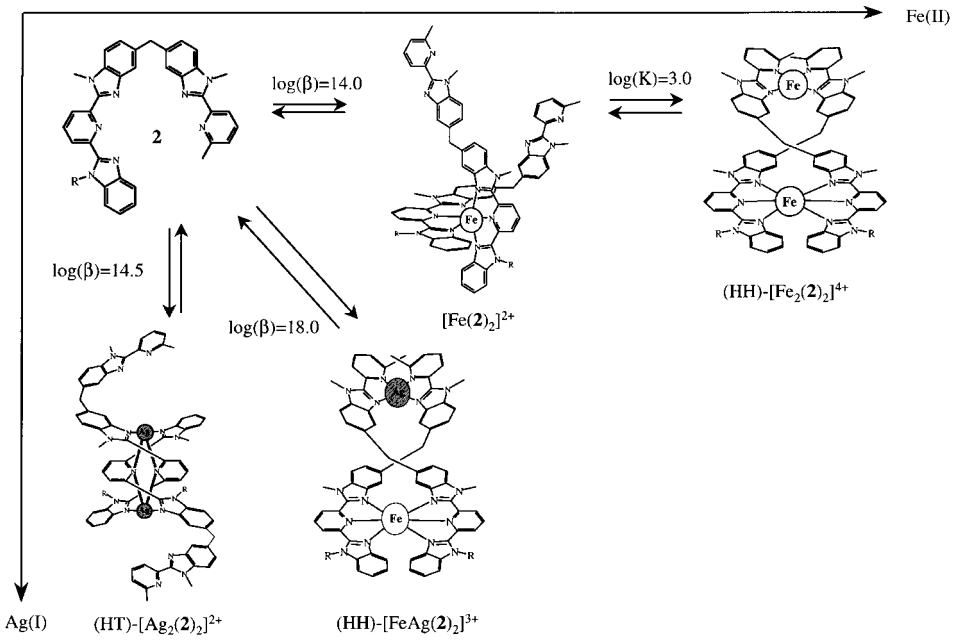

Figure 5. Thermodynamic self-assembly of (HH)-$[FeAg(\mathbf{2})_2]^{3+}$ in acetonitrile [9].

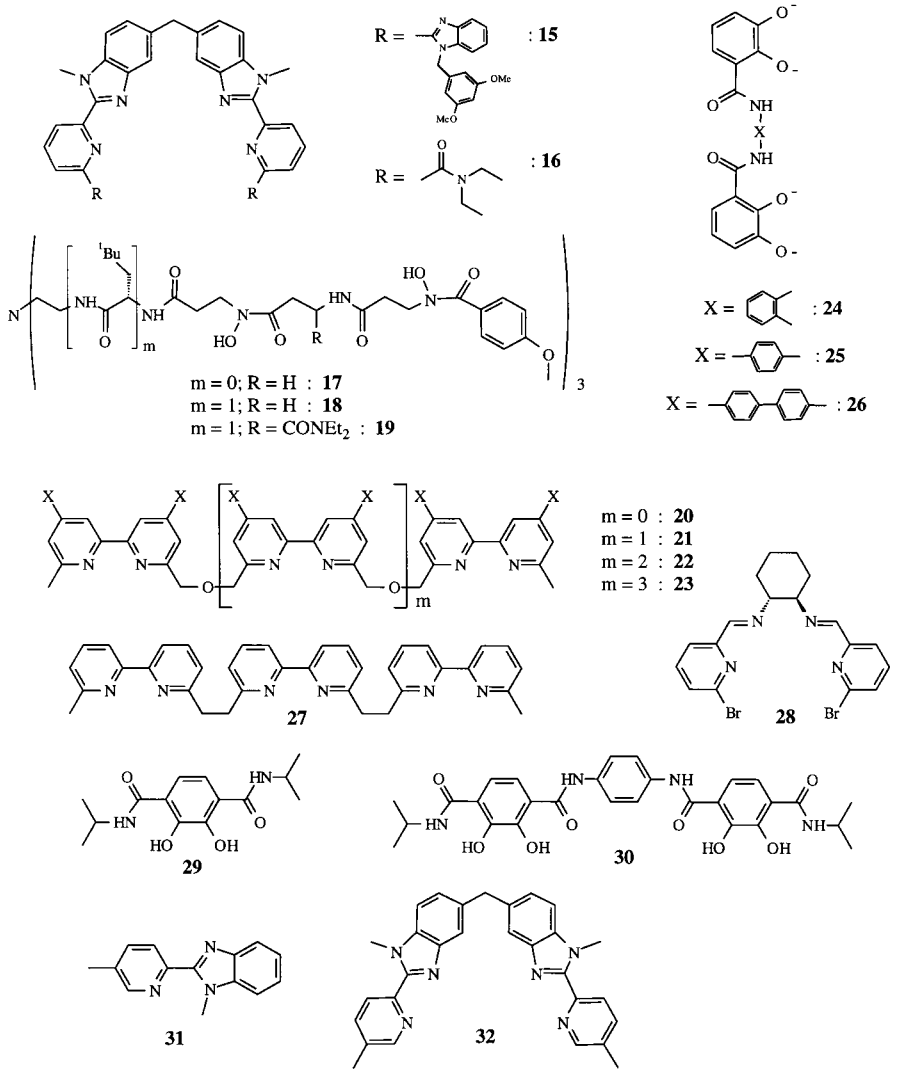

Chart 2.

tions of sterically constrained bipyridine- (**5**) or phenanthroline-containing ligand strands (**6**) show the positive cooperative formation of the double-stranded helicate $[Cu_2(\mathbf{5})_2]^{2+}$, but the generation of $[Cu_2(\mathbf{6})_2]^{2+}$ is not driven by positive cooperativity as a result of the increased distortion induced in the central aromatic spacer [12]. Alternatively, significant electrostatic repulsions between highly charged lanthanide metal ions (3+) are responsible for the negatively cooperative formation of the triple-stranded helicates $[Ln_2(\mathbf{15})_3]^{6+}$ and $[Ln_2(\mathbf{16})_3]^{6+}$ [24]. Detailed thermodynamic studies of the formation of related triple-stranded mometallic and dimetallic podates [Fe(**L**-3H)] and [Fe_2(**L**-6H)] (**L** = **17**–**19**) reveal drastically

different behaviours associated with only minor structural variations of the ligands [28]. [Fe_2(**18**-6H)] displays negative cooperativity for the successive coordination of two Fe(III), while a statistical process is observed for [Fe_2(**19**-6H)]. The residual carboxamide group in the latter ligand is thought to provide a belt of stabilizing interstrand hydrogen bonds in the final triple-helical complex. The shortening of the spacer between the tripodal anchor and the binding units in **17** strongly destabilizes the monometallic complex and leads to positive cooperativity for the complexation of the second metal in [Fe_2(**17**-6H)]. We conclude that (i) positive cooperativity is not systematically associated with helicate self-assembly and a judicious choice of specific conditional information can partially overcome the limiting thermodynamic factors associated with negative cooperativity and (ii) subtle interplay between structural, electronic and electrostatic effects strongly affects the enthalpic and entropic contributions of these processes. No simple and reliable correlations between the intrinsic informations encoded in the components and the thermodynamic characteristics of the final self-assembled helicate can be deduced from these pioneer works and, consequently no satisfying model currently exists for predicting helicate self-assembly. One major limitation concerns the modelisation and description of solvation effects associated with charged complexes and metal ions, but theoretical enthalpic and entropic considerations for much simpler neutral supramolecular hydrogen-bonded aggregates in organic solvents have been recently developed by Whitesides and coworkers [30] which offer promising perspectives for the related treatment of polymetallic coordination complexes and helicates. However, empirical approaches have been explored which have led to the recognition of remarkable self-recognition processes in solution.

(1) A mixture of oligo-bipyridines **20**–**23** possessing variable numbers of binding units exhibits self-recognition with Cu(I), thus providing selectively and quantitatively a mixture of polymetallic double-homostranded helicates $[Cu_n(\mathbf{L})_2]^{n+}$ (**L** = **20**, **21**, **22** and **23**, Equation (1)) [30].

$$2(\mathbf{20} + \mathbf{21} + \mathbf{22} + \mathbf{23}) + 14\ \mathrm{Cu(I)} \rightleftharpoons [Cu_2(\mathbf{20})_2]^{2+} + [Cu_3(\mathbf{21})_2]^{3+} + [Cu_4(\mathbf{22})_2]^{4+} + [Cu_5(\mathbf{23})_2]^{5+} \quad (1)$$

(2) A related recognition process shows the ligand strands **24**–**26**, which differ in the spacers between the two binding units, to give exclusively a mixture of dimetallic triple-homostranded helicates $[Ga_2(\mathbf{L})_3]^{6-}$ (**L** = **24**, **25** and **26**, Equation (2))[31].

$$3\ (\mathbf{24} + \mathbf{25} + \mathbf{26}) + 6\ \mathrm{Ga(III)} \rightleftharpoons [Ga_2(\mathbf{24})_3]^{6-} + [Ga_2(\mathbf{25})_3]^{6-} + [Ga_2(\mathbf{26})_3]^{6-} \quad (2)$$

However, a less drastic structural variation of the spacers in the ligands **21** (oxopropylene bridges) and **27** (ethylene bridges) provides only partial recognition upon reaction with Cu(I) [32]. Although a significant destabilization of the double-heterostranded helicate $[Cu_3(\mathbf{21})(\mathbf{27})]^{3+}$ is expected, it still corresponds to 20% of the ligand speciation in the final mixture [32].

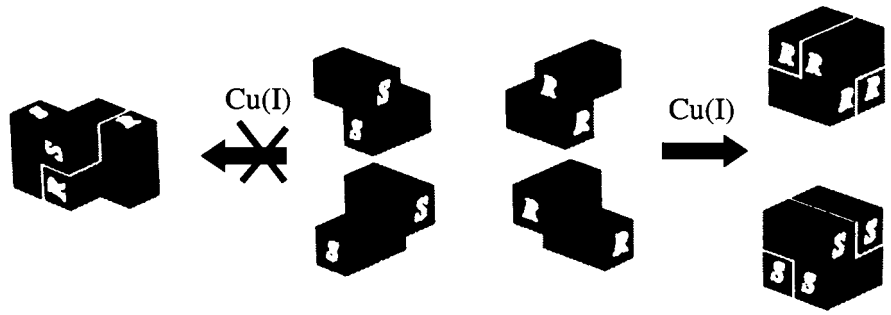

Figure 6. Thermodynamic self-recognition of chiral ligands in the double-stranded helicates $[Cu(\mathbf{28})_2]^{2+}$. The cube-shaped species is more compact [33]. (Reproduced with the permission from Ref. [33]. Copyright 1998 WILEY-VCH Publishers.)

(3) In this context, one may be surprised that a mixture of the chiral strands *RR*-**28** and *SS*-**28**, which only differ in the absolute configurations of two stereogenic centers in the spacer, produces selectively a single racemic pair of homochiral double-stranded helical enantiomers with Cu(I) (Equation (3)) [33]. Stack and coworkers have demonstrated that the two stereogenic carbons in **28** control the orientation of the binding units leading to optimum intramolecular van der Waals interactions for homochiral arrangements of the ligands in the final helicate (Figure 6).

$$2(RR\text{-}\mathbf{28} + SS\text{-}\mathbf{28}) + 4\text{Cu(I)} \leftrightharpoons \Lambda\Lambda\text{-}[\text{Cu}_2(RR\text{-}\mathbf{28})_2]^{2+} + \Delta\Delta\text{-}[\text{Cu}_2(SS\text{-}\mathbf{28})_2]^{2+} \quad (3)$$

Related maximization of hydrophobic effects may be tentatively invoked to rationalize the rather systematic exclusive formation of a single diastereomeric helicate from enantiopure ligands and metal ions [2, 5, 34].

As previously mentioned, reliable thermodynamic investigations of helicate self-assembly are rare, but related kinetic studies are almost completely absent except for one paper published by Lehn and coworkers reporting the slow kinetic formation of the pentametallic double-stranded helicate $[Cu_5(\mathbf{23})_2]^{5+}$ [35]. Complicated competitive mechanistic pathways have been invoked together with an unusual trimetallic hairpin-shaped intermediate, but no kinetic constants have been extracted from these data. On the other hand, the helical interconversion (or helical racemization, Equation (4)) have been investigated in more detail because kinetic parameters can be easily obtained from simple variable temperature NMR experiments using diastereotopic protons or carbons [23, 36–38] or CD spectra [38].

$$\Lambda\Lambda\text{-}[\text{M}_2(\mathbf{L})_i]^{n+} \leftrightarrow \Delta\Delta\text{-}[\text{M}_2(\mathbf{L})_i]^{n+} \quad (i = 2, 3) \quad (4)$$

Raymond and coworkers found that the helical interconversions of the monometallic complex $[Ga(\mathbf{29}\text{-}2H)_3]^{3-}$ and the dimetallic triple-stranded helicate $[Ga_2(\mathbf{30}\text{-}4H)_3]^{6-}$ follow intramolecular Bailar twists without bond breaking [36]. The

similar activation energies found for the two complexes ($\Delta G^{\neq}_{298} = 79$ kJ/mol for $[Ga_2(\mathbf{30}\text{-}4H)_3]^{6-}$ and $\Delta G^{\neq}_{298} = 67$ kJ/mol for $[Ga(\mathbf{29}\text{-}2H)_3]^{3-}$) involve the formation of the 'meso' intermediate $\Lambda\Delta$-$[Ga_2(\mathbf{30}\text{-}4H)_3]^{6-}$ during the helicate interconversion. This mechanism has been confirmed later for related dimetallic and trimetallic Ti(IV)-helicates [37], but parallel investigations with ligands **31** and **32** and Co(II) lead to the opposite conclusion: the very slow racemization process ($\Delta G^{\neq}_{298} = 101$ kJ/mol) of the triple-stranded helicate $[Co_2(\mathbf{32})_3]^{4+}$ involves bond breaking and the decomplexation of one metal ion according to Equation (5) [38].

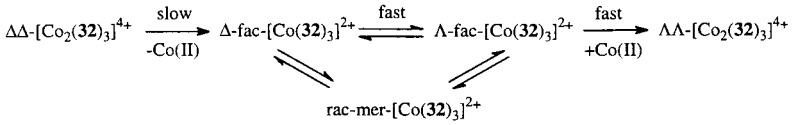

(5)

The apparent discrepancy between these results has been tentatively solved by Williams [5, 39] who points out that the latter complex $[Co_2(\mathbf{32})_3]^{4+}$ cannot reach the trigonal prismatic geometry required for the Bailar twist as a result of severe steric restrictions imposed by (i) the rigid aromatic diphenylmethane spacer and (ii) the significant ligand field of the non-spherical d^7 configuration of Co(II). For $[Ga_2(\mathbf{30}\text{-}4H)_3]^{6-}$, the less rigid spacer and the spherical Ga(III) ion allow the fast intramolecular Bailar twist and no decomplexation is required. One may conclude that a careful design of the spacing group is a promising tool for controlling the lability of helicate racemization in view of their use as chiral building blocks.

2. Some Structural Alternatives to Helicates

As an extension of the work initiated with helicates, the design of complexes with predetermined metal to ligand ratio generated by metal-assisted self-assembly has attracted much recent interest. Successful assemblies of polymetallic grids [39]. racks [40], polygons and boxes [41], cylinders [42] and metallacrowns [43] have demonstrated the great potentiality of a judicious combination of intrinsic information borne by the reacting components, i.e. the ligand strands and the metal ions (Figure 7). However, our current description and understanding of thermodynamic self-assembly of metallosupramolecular complexes is so partial (*vide supra*) that the actual stoichiometry (for instance $[M_nL_n]$, n = 2, 3, 4 ...) and the geometrical arrangement of the ligands in the final supramolecular complex cannot be safely predicted. Several structural alternatives to helicates which can coexist under thermodynamic equilibria, have been observed and characterized either by accident, by chance or by design leading to new classes of structurally attractive metallosupramolecular complexes (circular helicates, catenates, cages). However, the development of a preconceived and organized final architecture remains one of the ultimate goals of self-assembly and this requires an improved understanding of the structural and electronic factors which control the formation of the final complexes.

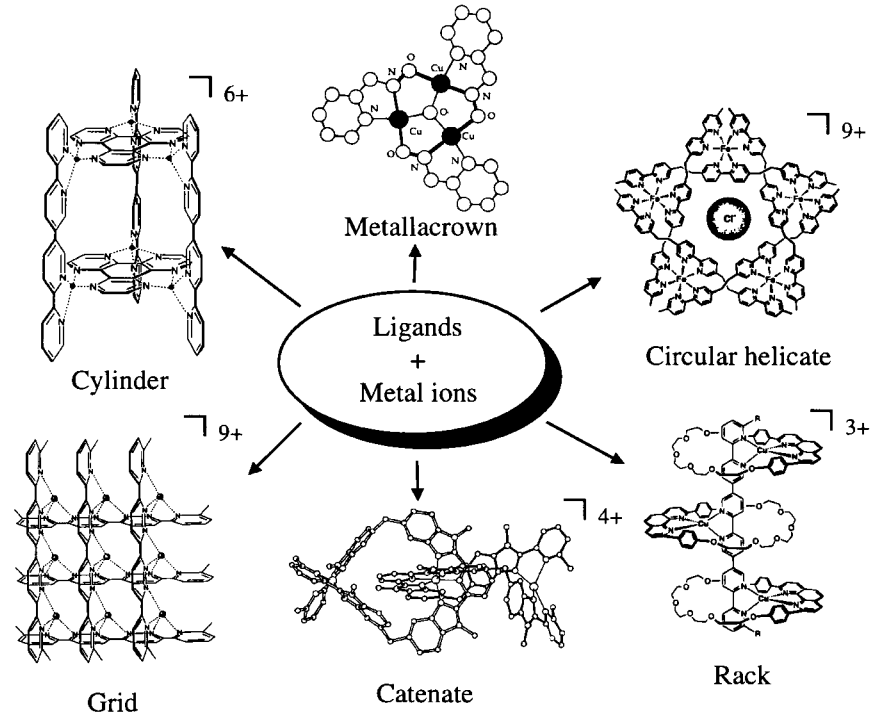

Figure 7. Selected metallosupramolecular complexes obtained by self-assembly.

2.1. SELF-ASSEMBLED ORGANOMETALLIC CATENATES RELATED TO DOUBLE-STRANDED HELICATES

In an effort to prepare heteropolymetallic double-stranded helicates, Piguet and coworkers have synthesised the heterotritopic ligand **33** whose bidentate binding units are coded for the recognition of tetrahedral Ag(I) and the tridentate binding unit coded for octahedral Fe(II) [9]. Upon reaction with stoichiometric amounts of Fe(II) (0.5 eq) and Ag(I) (1 eq), a single complex of stoichiometry $[FeAg_2(\mathbf{33})_2]^{4+}$ was identified in solution whose NMR spectrum is compatible with the expected D_2-symmetrical double-stranded helicate [44]. However, two types of dark violet crystals with different morphologies (hexagonal prisms and pellets) can be isolated and their crystal structures reveal the existence of two unexpected diastereomers: the pellets contain racemic pairs of D_2-symmetrical homochiral [2]-catenate (*PP*-$[FeAg_2(\mathbf{33})_2]^{4+}$ and *MM*-$[FeAg_2(\mathbf{33})_2]^{4+}$) and the hexagonal prisms consist of the heterochiral S_4-symmetrical meso form PM-$[FeAg_2(\mathbf{33})_2]^{4+}$ (Figure 8) [44]. Detailed investigations in solution using variable temperature NMR and NOE effects eventually established that the catenate structure made of two helically wrapped and interlocked organometallic macrocycles is maintained in solution, but fast dynamic processes interconvert the various diastereomers in acetonitrile. Molecular mechanics suggests that the interlocked structure of $[FeAg_2(\mathbf{33})_2]^{4+}$ results

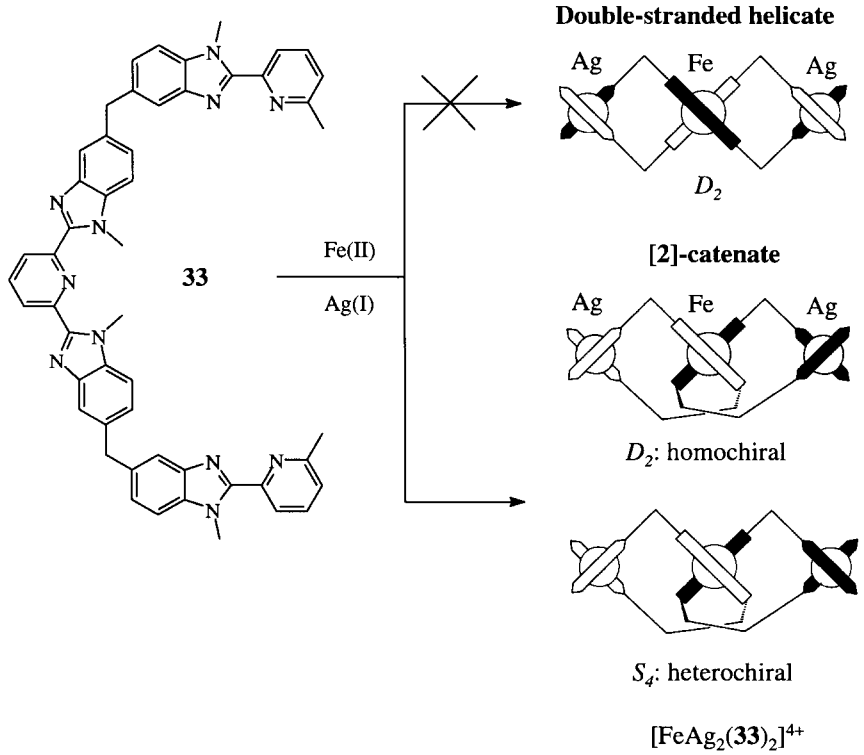

Figure 8. Self-assembly of the heterotrimetallic [2]-catenate $[FeAg_2(\mathbf{33})_2]^{4+}$ instead of the expected double-stranded helicate [44].

from steric constraints in the diphenylmethane spacer which prevent the formation of a linear helicate. Self-assembled catenates can be thus considered as topological isomers of double-stranded helicates which maintain a mono-dimensional arrangement of the metal ions.

A related approach has been recently developed by Sauvage and coworkers for the preparation of inert heterotrimetallic organometallic catenates [46]. The segmental tridentate-bidentate-tridentate ligand strands **34** have been reacted stepwise with Ru(II) and Cu(I) to give $[Ru_2Cu(\mathbf{34})_2]^{5+}$ where two inert Ru(II) metal ions clip the two interlocked organometallic macrocycles (Figure 9). According to this synthetic strategy, the formation of an inert *pseudo*-octahedral Ru(II) intermediate prevents thermodynamic equilibria to occur and the final complex $[Ru_2Cu(\mathbf{34})_2]^{5+}$ does not necessarily correspond to the most stable complex which can be formed between **34**, Ru(II) and Cu(I) in contrast to $[FeAg_2(\mathbf{33})_2]^{4+}$ which is the thermodynamic product of a strict self-assembly process.

For segmental ligands with long and flexible spacers between the binding units, the coordination of two successive binding segments to the same metal ion has been observed [46] leading to a doubly-looped structure in $[Fe_3(\mathbf{35})_2]^{4+}$ [47]. In the latter complex, the three metals lie on a line: the two terminal Fe(II) are *pseudo*-

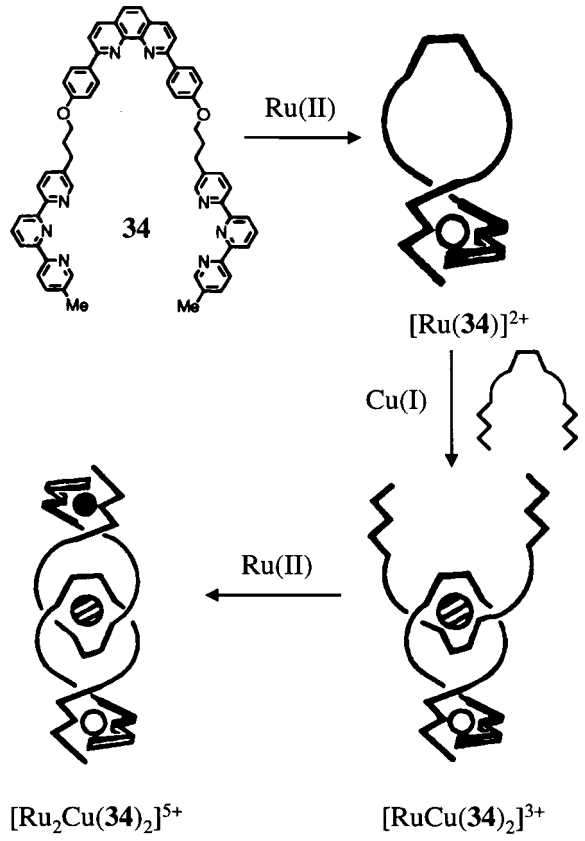

Figure 9. Stepwise synthesis of an inert heterotrimetallic [2]-catenate [45].

octahedrally coordinated by the central and one terminal tridentate binding unit of the same strand, thus leaving one terminal tridentate binding unit on each strand unoccupied for its meridional complexation to the third Fe(II).

2.2. SELF-ASSEMBLED CIRCULAR HELICATES RELATED TO DOUBLE- AND TRIPLE-STRANDED HELICATES

For the self-assembly of a helicate $[M_nL_m]^{z+}$, the relative metal to ligand stoichiometric ratio (n/m) is easily accessible by a combination of various usual analytical and spectroscopic techniques (spectrophotometry, potentiometry, vapor phase osmometry, NMR, etc. ...) [2], but a reliable determination of the absolute values of n or m are often difficult to obtain and Electrospray-MS (ES-MS) in solution [48] and X-ray diffraction in the solid state have been systematically used to address this problem. As early as in 1994, the detailed investigation of positively charged helicates by ES-MS in solution has led Hopfgartner, Piguet and coworkers to propose that the expected helicate does not systematically correspond to the

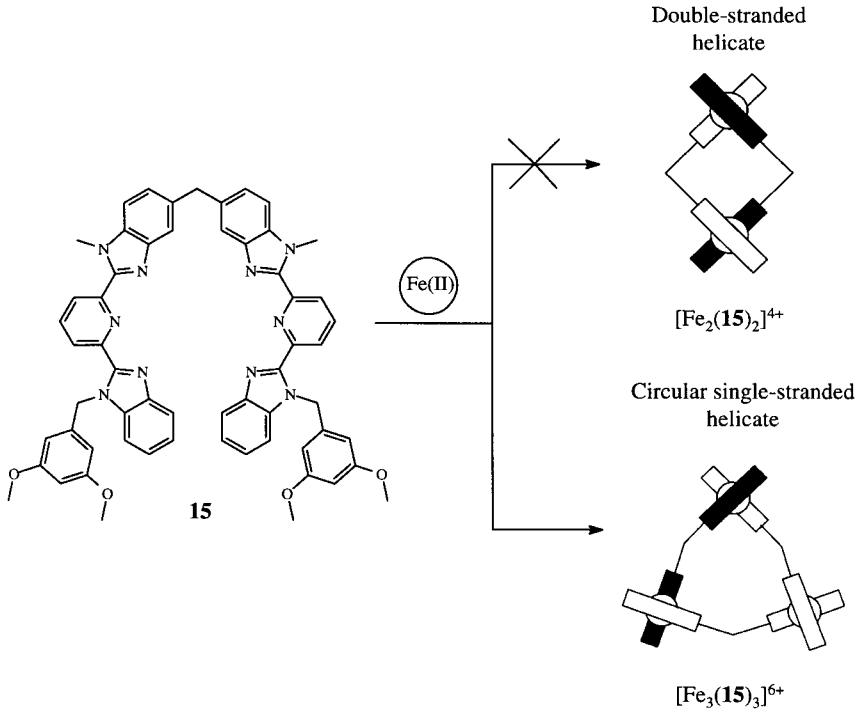

Figure 10. Self-assembly of the cicular single-stranded helicate $[Fe_3(\mathbf{15})_3]^{6+}$ instead of the expected double-stranded helicate [48]. (Reproduced with the permission from Ref. [2]. Copyright 1997 American Chemical Society.)

product formed in solution [48]. It has been shown that ligand **15** reacts with octahedral metal ions Fe(II), Co(II) and Ni(II) to give mixtures of the expected double-stranded helicate $[M_2(\mathbf{15})_2]^{4+}$ (n/m = 1) together with a second complex possessing the same ligand to metal ratio: $[M_3(\mathbf{15})_3]^{6+}$. The relative quantity of each complex in solution depends on the selected metal ion and the latter complex is selectively and quantitatively formed for Fe(II) thus allowing its characterization by NMR in solution as a D_3-symmetrical single-stranded circular helicate (Figure 10) [49]. These observations have initiated an intense research activity which aims at elucidating the factors responsible for the formation of circular helicates over linear ones [22, 49–55].

Related assembly processes with ligands **36** and **37** produce mixtures containing variable proportions of oligomers $[Fe_n(\mathbf{36})_n]^{2n+}$ (n = 3, 4) [49] and $[Cu_n(\mathbf{37})_n]^{n+}$ (n = 2–4) [22]. For the latter mixture, a NMR titration in CD_2Cl_2 displays relative ratios of 6 : 4 : 3 for complexes with n = 2, 3 and 4 respectively, while fast dynamic interconversions on the NMR time scale prevent the characterisation in CD_3NO_2 and CD_3CN [22]. It is worth noting that upon crystallisation the equilibrating mixture is quantitatively converted into the formation of the double-stranded helicate $[Cu_2(\mathbf{37})_2](PF_6)_2$ which corresponds to the less solu-

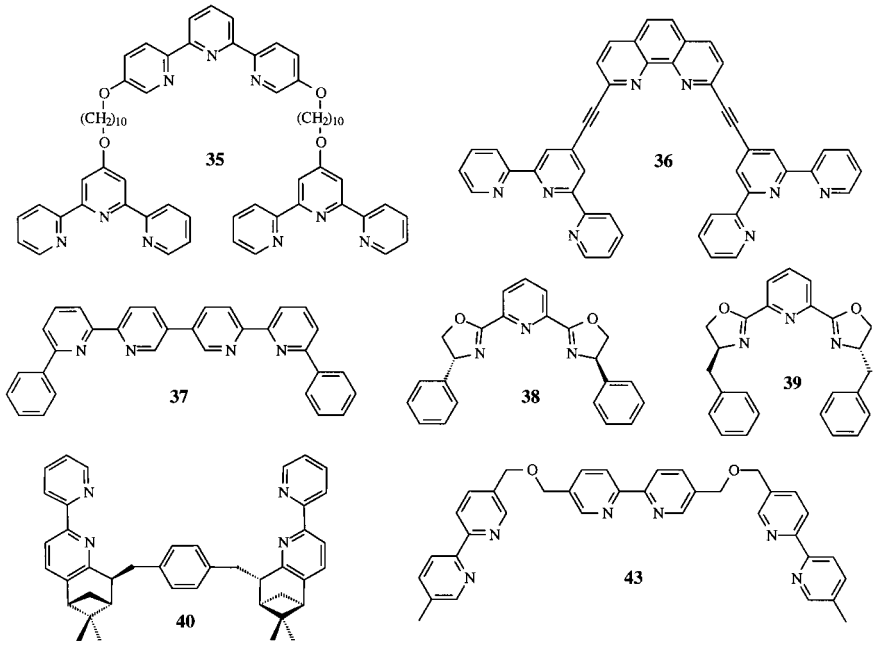

Chart 3.

ble complex under these conditions. Very similar processes have been postulated for the reaction of the enantiopure ligands **38**, **39** [50] and **40** [51] with Ag(I). The thermodynamic equilibria are shifted upon crystallisation leading to the isolation of a single diastereomer in each case: circular single-stranded helicates (*P*)-$[Ag_3(\mathbf{38})_3]^{3+}$ [50] and (*P*)-$[Ag_6(\mathbf{40})_6]^{6+}$ and a double-stranded helicate (*P*)-$[Ag_2(\mathbf{39})_2]^{2+}$ [50]. Interstrand π-stacking interactions, observed in the crystal structure of (*P*)-$[Ag_3(\mathbf{38})_3]^{3+}$, have been invoked to rationalize its selective formation, but the partial dissociation of the trimer in solution to give the double-stranded helicate $[Ag_2(\mathbf{38})_2]^{2+}$ implies that other effects affect the distribution of complexes in solution.

Polymetallic circular single-stranded helicates $[M_nL_n]^{z+}$ ($n > 2$) can be considered as a two-dimensional extension of the dimetallic double-stranded helicates $[M_2L_2]^{z+}$. Applying this reasoning to dimetallic triple-stranded helicate $[M_2L_3]^{z+}$ (n/m = 0.67) leads to the conclusion that no regular circular helicate is compatible with this stoichiometric ratio. A two-dimensional arrangement of an even number of metal ions connected by ligand strands with n/m = 0.67 requires alternated single- and double-stranded bridges between the metals. To the best of my knowledge, the crystal structure of the octametallic circular alternated single/double-stranded helicate $[Co_8(\mathbf{41})_{12}(ClO_4)]^{3+}$ represents the unique report in which an extended circular oligomer is obtained instead of the expected triple-stranded helicate $[Co_2(\mathbf{41})_3]^{+}$ (Figure 11) [52]. A perchlorate anion is encapsulated within the organometallic cavity and a template effect operating during the crys-

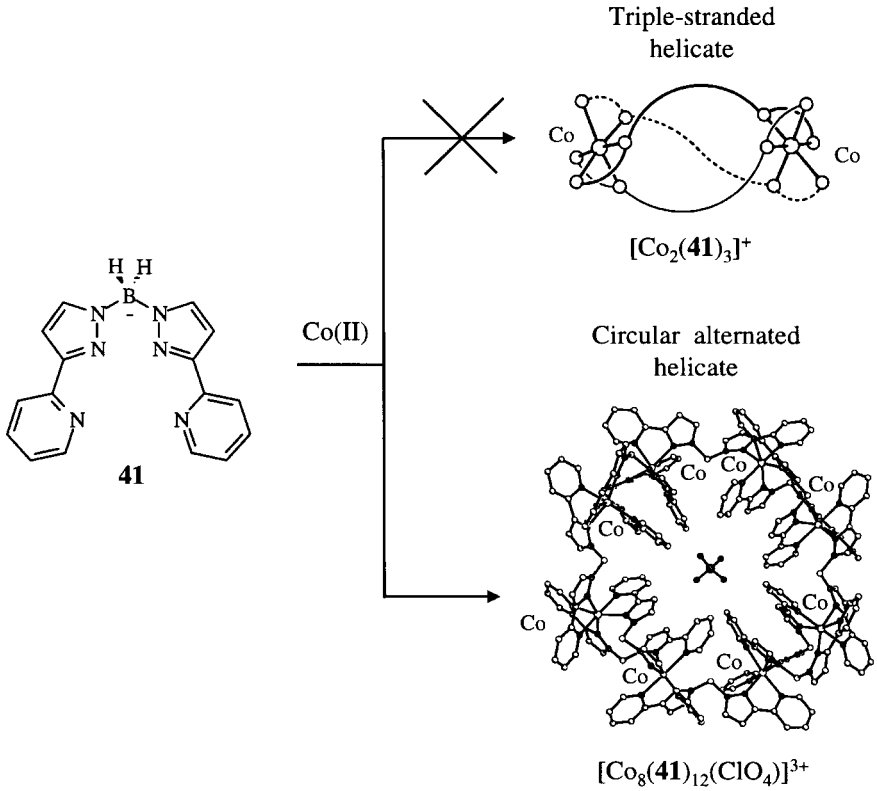

Figure 11. Self-assembly of the octametallic alternated circular helicate $[Co_8(\mathbf{41})_{12}(ClO_4)]^{3+}$ instead of the expected triple-stranded helicate [52].

tallisation process has been proposed. Although the solution structure has not been solved, preliminary results indicate that the circular structure is not maintained [52].

In the trimetallic triple-stranded helicate $[Ni_3(\mathbf{42})_3]^{6+}$, a relative stoichiometric ratio $n/m = 1$ is restored [53] which is compatible with the formation of two-dimensional extended polymetallic circular double-stranded oligomers for $m = n > 3$ (Figure 12) [54]. Upon reaction of **42** with $FeCl_2$, the circular double-stranded (i.e. each metal ion is connected to its neighbours by two wrapped strands) helicate $[Fe_5(\mathbf{42})_5Cl]^{9+}$ is formed and it has been first characterized in the solid state by using X-ray diffraction [54]. A subsequent detailed analysis of the assembly process in solution [55] reveals that (i) the expected triple-stranded helicate $[Fe_3(\mathbf{42})_3]^{6+}$ is observed as a transcient intermediate and (ii) the nature of the counter anion is crucial for controlling the stoichiometry of the final complexes. The chloride anion acts as a template for the formation of the pentametallic circular helicate and remains encapsulated within the organometallic cavity in the solid state. The larger SO_4^{2-} and SiF_6^{2-} anions favour the formation of a larger

cavity leading to the quantitative formation of the hexametallic circular double-stranded helicate $[Fe_6(\mathbf{42})_6]^{12+}$. The intermediate size of the bromide anion gives the expected mixture of penta- and hexametallic complexes in solution. A minor modification of the spacer in **43** severely affects the product distribution leading to the exclusive formation of the tetrametallic double-stranded circular helicate $[Fe_4(\mathbf{43})_4]^{8+}$ whatever the nature of the counter anions [55].

2.3. SELF-ASSEMBLED METALLOSUPRAMOLECULAR CAGES RELATED TO TRIPLE-STRANDED HELICATES

Extended tri-dimensional arrangements of metal ions in supramolecular tetrahedral cages $[M_4L_6]^{z+}$ (n/m = 0.67) result from the assembly of bis-bidentate ligands with octahedral metal ions; a process usually used for the preparation of dimetallic triple-stranded helicates $[M_2L_3]^{z+}$ which possess the same relative metal to ligand ratio. If we neglect solvation effects, the dominant translational entropic contributions systematically favour the formation of the triple-stranded helicate which contains only five components compared to ten for the supramolecular cage [29]. However, minor structural constraints within the ligand backbone can provide opposite enthalpic contributions which overcome the entropic trend eventually leading to the formation of the supramolecular cages [56]. Saalfrank and coworkers first reported the generation of 'adamantoid' tetrahedral cages $[M_4(\mathbf{44})_6]^{4-}$ (M = Mg, Mn, Co, Ni, Zn) [58] and $NH_4[Fe_4(\mathbf{44})_6]$ [59], in which the corners are occupied by pseudo-octahedral metal ions and the six vertices of the tetrahedron are constituted by the bis-bidentate strands (Figure 13). In similar processes, the related ligand strands **45**–**47** produce selectively tetrahedral cages $[M_4(\mathbf{45})_6]$ and $[M_4(\mathbf{46})_6]^{12-}$ (M = Ga(III), Fe(III)) [56] and $[Co_4(\mathbf{47})_6]^{8+}$ [59] respectively. The preference for the formation of the tri-dimensional tetrahedral cage over the mono-dimensional triple-stranded helicate has been analysed by Raymond and coworkers in terms of the relative orientations of the binding units toward the threefold axis of the pseudo-octahedral coordination sites [57]. The use of divergent bis-bidentate binding units in **44**–**47** which are not compatible with the formation of linear helicates is a prerequisite for the design of the final supramolecular cage.

A fascinating fine tuning of steric effects has been recently reported by Stack and coworkers [61]. The achiral ligand **48** reacts with Ga(III) to give the expected dimetallic triple-stranded helicate $[Ga_2(\mathbf{48})_3]^{6-}$ [61], while the chiral analogue *SS*-**49** where two hydrogen atoms of the spacer are replaced by methyl groups, produces quantitatively the tetrahedral cage $[Ga_4(SS\text{-}\mathbf{49})_6]^{12-}$. A detailed geometrical analysis concludes that unfavorable synclinal interactions between the methyl groups of the spacer and the amide functions are removed in the tetrahedral cage [60]. As previously demonstrated for the double-stranded helicates $[Cu_2(\mathbf{28})_2]^{2+}$ [33], the optimization of intramolecular hydrophobic interactions induces a high diastereoselectivity leading to the exclusive generation of a single pair of homochiral

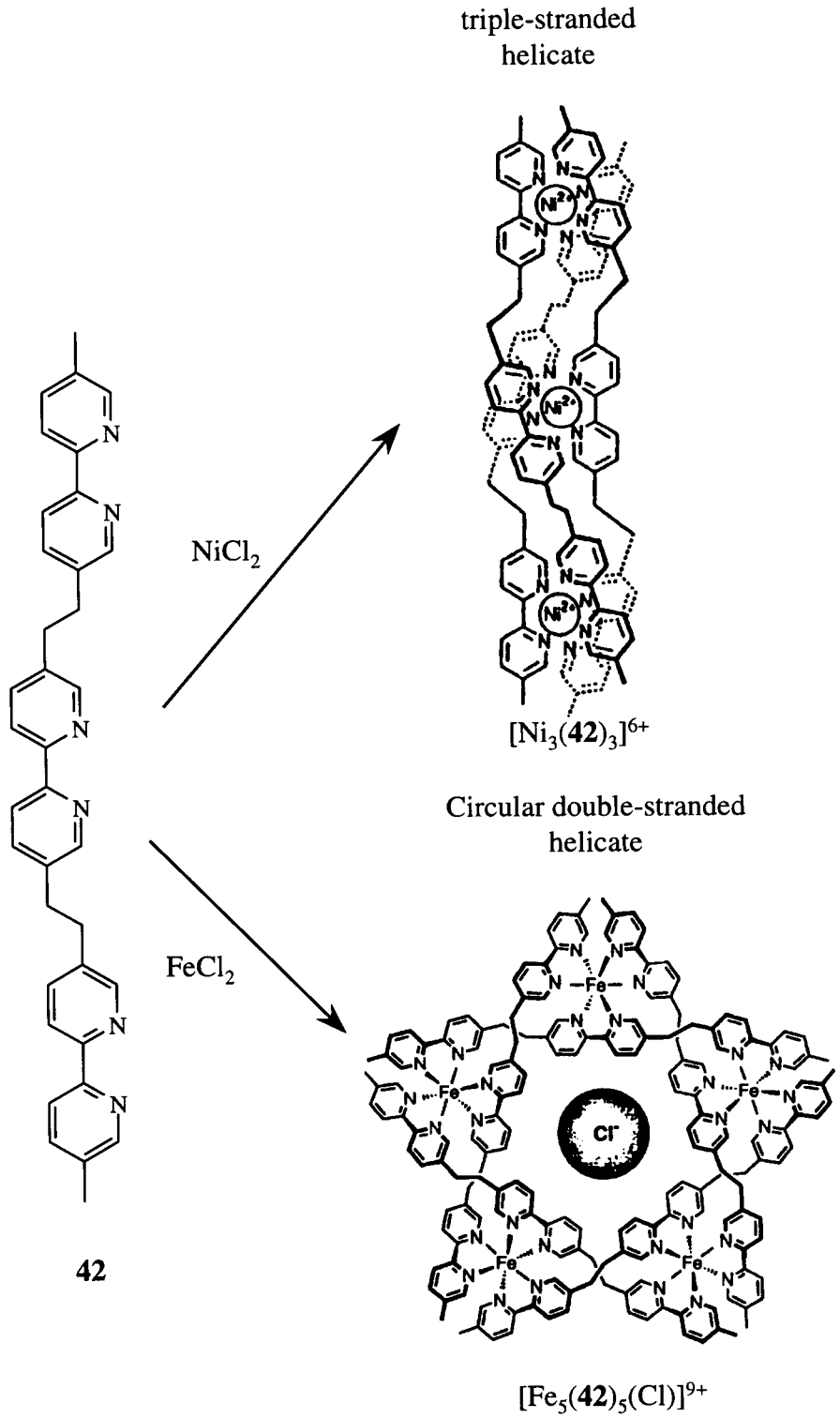

Figure 12. Self-assembly of a triple-stranded helicate $[Ni_3(\mathbf{42})_3]^{6+}$ and a pentametallic circular double-stranded helicate $[Fe_5(\mathbf{42})_5(Cl)]^{9+}$ [54].

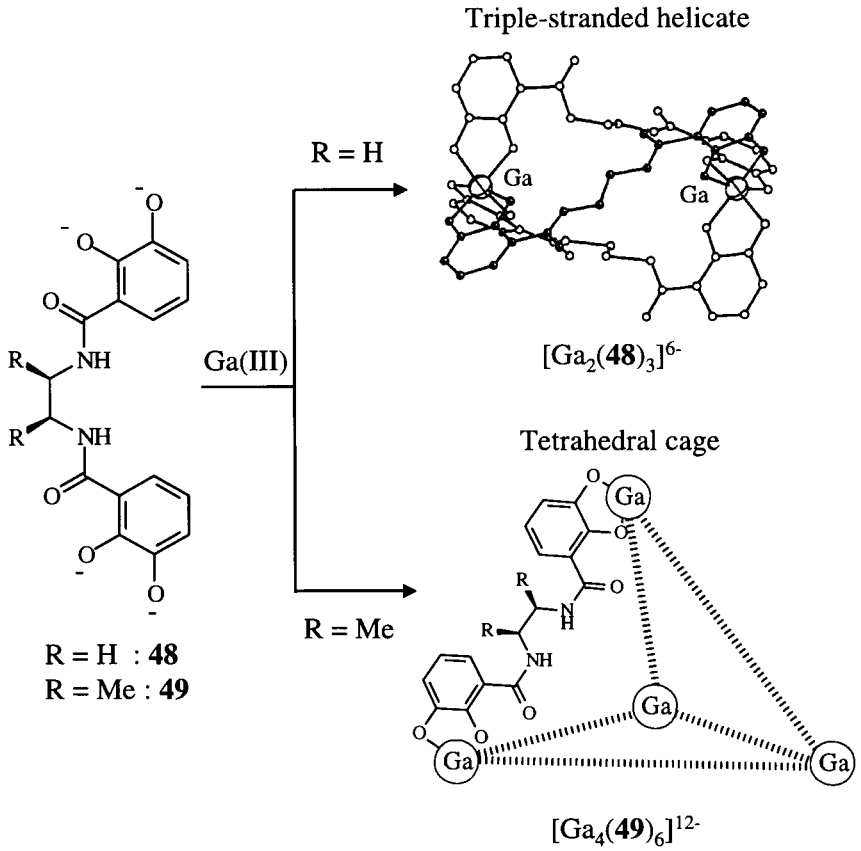

Figure 13. Self-assembly of a triple-stranded helicate $[Ga_2(\mathbf{48})_3]^{6-}$ and a supramolecular tetrahedral cage $[Ga_4(\mathbf{49})_6]^{12-}$ [60].

enantiomer upon reaction of a racemic mixture of ligands with Ga(III) (Equation (6)).

$$6(RR\text{-}\mathbf{49} + SS\text{-}\mathbf{49}) + 8\text{Ga(III)} \leftrightarrow \Lambda\Lambda\Lambda\Lambda\text{-}[Ga_4(SS\text{-}\mathbf{49})_6]^{12-} + \Delta\Delta\Delta\Delta\text{-}[Ga_4(RR\text{-}\mathbf{49})_6]^{12-} \quad (6)$$

3. The Future of Helicates: Applications and New Building Methods

Despite the limited thermodynamic control of metallosupramolecular self-assembly, the design of preconceived linear homotopic double- and triple-stranded helicates has become a rather straightforward synthetic process which can be roughly rationalized using the intrinsic information encoded in the components. Recent intensive activities have been focused on the physical and chemical applications of these new available supramolecular edifices according to three main

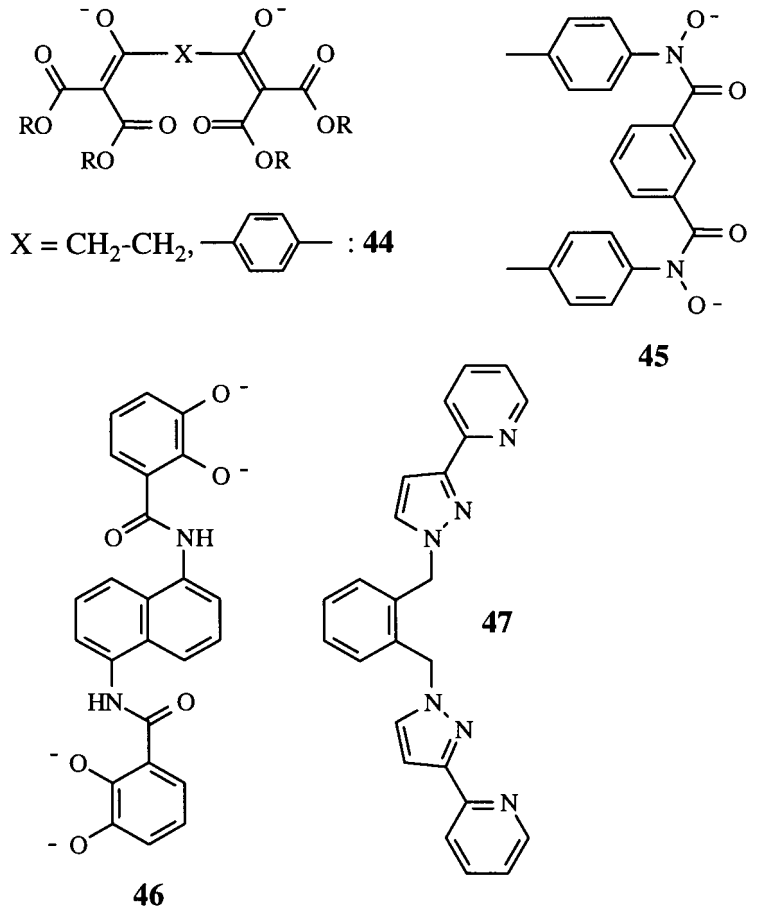

Chart 4.

lines: (1) the development of chiral hosts [62], (2) the design of polymetallic supramolecular functional devices [63] and (3) the design of template agents for the preparation of topologically non-trivial molecules such as trefoil knots and related systems [64], and chiral podand receptors for lanthanide metal ions [65].

3.1. HELICATES AS SELF-ASSEMBLED SUPRAMOLECULAR HOSTS

The assembly of a dimetallic *double-stranded* helicate provides a helical metal-containing *macrocyclic* cavity, while the formation of a dimetallic *triple-stranded* helicate is associated with the production of a related *macrobicyclic* cavity (Figure 14). The related *circular* helicates produce internal *toroidal* cavities similar to those found in metallacrowns [43]. The complexing properties of these self-assembled cavities strongly depend on (i) the possible interactions between the spacer and the guest (van der Waals, dative bonds, electrostatic, etc. . . .) and (ii) the

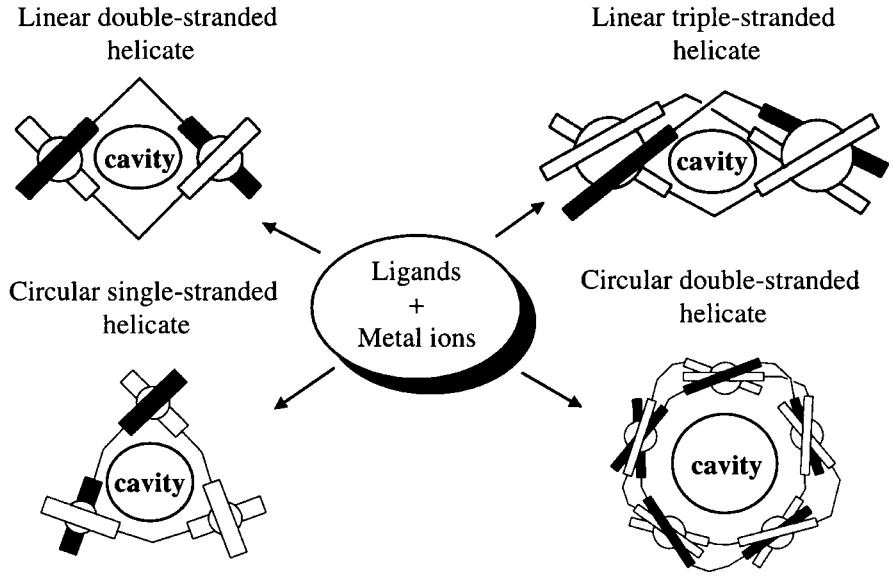

Figure 14. Metal-containing macrocyclic and macrobicyclic cavities in self-assembled linear and circular helicates.

electrostatic charge borne by the helicate. Negatively charged triple-stranded helicates $[Ti_2\mathbf{L}_3]^{4-}$ (**L = 50–52**) incorporate alkaline cations into their macrobicyclic cavities in the solid state and in solution [66], while the positively charged circular double-stranded helicates $[Fe_5(\mathbf{42})_5]^{10+}$ and $[Fe_6(\mathbf{42})_6]^{12+}$ have been shown to interact with anions [54, 55]. Template effects involving the ionic guest have been invoked to explain the selective formation of linear triple-stranded helicates [66] and circular double-stranded helicate [54, 55], but no convincing investigations of the mechanisms leading to the final architectures have been reported.

In an effort to control the complexation of the internal guest, Saalfrank and coworkers prepared the two related ligand strands **53** and **54** [68]. Suprisingly, **53** produces the expected racemic mixture of left- and right-handed triple-stranded helicates $[Fe_2(\mathbf{53})_3]$, but the pyridine containing ligand **54** gives the achiral side-by-side complex *PM*-$[Fe_2(\mathbf{54})_3]$ (i.e. the 'meso' form). Structural investigations in the solid state and in solution reveal that the pyridine groups of the spacers in the latter complex strongly favour the coordination of K^+ in the macrobicyclic cavity leading to the correct formulation *PM*-$[K \subset Fe_2(\mathbf{54})_3]^+$ for the final complex. Alternatively, van der Waals interactions between stacked aromatic rings have been used by Harding and coworkers for complexing neutral organic guests [69, 70]. The electron-deficient naphthalene-tetracarboxamide spacers of ligand **55** are ideally suited to strongly interact with electron-rich substrates. In the self-assembled double-stranded helicate $[Zn_2(\mathbf{55})_2]^{4+}$, their face-to-face arrangement provides a hydrophobic macrocyclic cavity which strongly bind *o*-dimethoxybenzene [68] and dinaphthol guests [69].

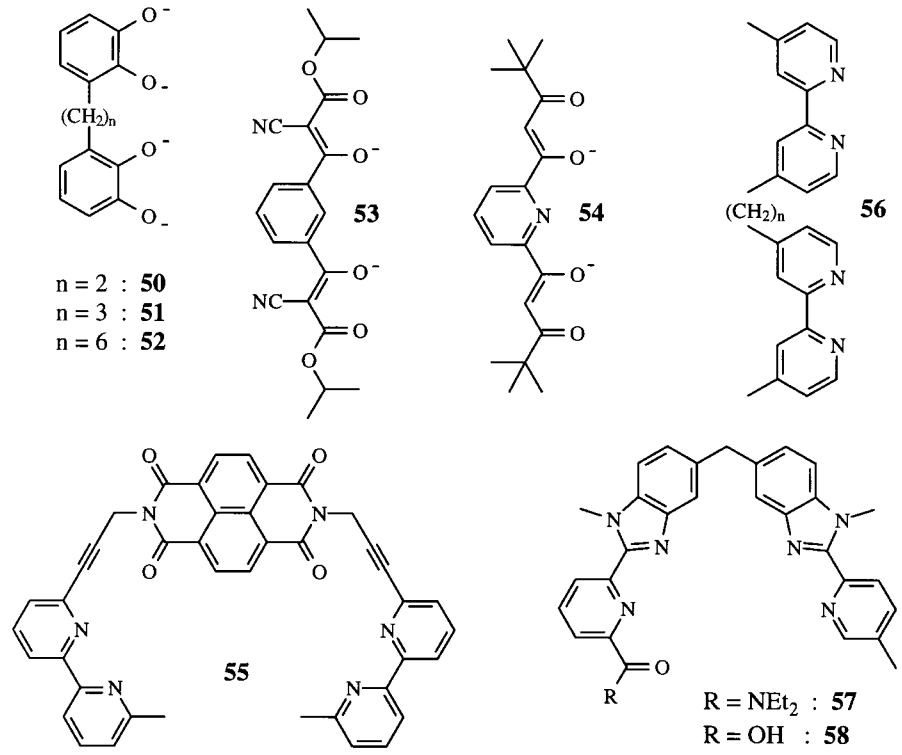

Chart 5.

3.2. HELICATES AS SUPRAMOLECULAR FUNCTIONAL DEVICES

Although it has been early recognized that different metal ions can be selectively introduced into heterometallic helicates [2], only a few attempts have been made to exploit the fascinating magnetic, electronic and optical properties of organized polymetallic complexes for the design of functional devices. This is particularly striking for helicates with d-block metal ions because several hundreds of polymetallic complexes have been reported, but, to the best of my knowledge, the triple-stranded helicate $[RuFe(\mathbf{56})_3]^{4+}$ is the only one for which a precise function (directional Ru → Fe energy transfer) has been described [70]. The reverse situation is found with lanthanide metal ions (4f-block) which are difficult to introduce into organized architectures (less than ten lanthanide-containing helicates have been isolated and characterized), but whose peculiar electronic, magnetic and spectroscopic properties have been systematically exploited for the design of functional devices. In 1993, Piguet and cowokers reported that nine-coordinate tricapped trigonal prismatic 4f-block metal ions can produce self-assembled dimetallic triple-stranded helicates $[Ln_2(\mathbf{15})_3]^{6+}$ with bis-tridentate segmental ligands [24]. The introduction of Ln = Eu(II) or Tb(III) as long-lived luminescent stains provides light-converting devices in which UV light is efficiently collected by the aro-

matic groups of the ligand (via Laporte-allowed $\pi \rightarrow \pi^*$ transitions), energy is then transfered from the periphery of the helicate toward the central metal ions which re-emit visible light on the millisecond time scale (the *Antenna* effect). The efficiency of the overall UV $\rightarrow$ vis conversion process is strongly limited by low-lying $^3\pi\pi^*$ and LMCT (for Ln = Eu) excited states which quench the luminescence process. However, the residual emission is sufficient to evidence an intramolecular Tb $\rightarrow$ Eu energy transfer along the helical axis in the heterodimetallic complex $[TbEu(\mathbf{15})_3]^{6+}$ which can find applications for directional light-conversion and the preparation of rare earth four-levels lasers (Figure 15a) [24]. The replacement of the terminal benzimidazole side arms in **15** by carboxamide groups in **16** significantly improves the stability and the emission properties of the final helicate $[Eu_2(\mathbf{16})_3]^{6+}$, thus allowing a simultaneous tuning of electronic and thermodynamic properties [24].

The connection of a bidentate binding unit coded for the recognition of octahedral d-block metal ions with an unsymmetrical tridentate binding unit coded for the recognition of 4f-block ions in ligand **57** allows the selective preparation of heterodimetallic head-to-head triple-stranded helicates (HHH)-$[LnM(\mathbf{57})_3]^{5+}$ (M = Zn, Fe, Co) [25, 26, 65]. Each metal ion is located in a coordination site which satisfies its stereochemical requirements: *pseudo*-octahedral for M(II) and *pseudo*-tricapped trigonal prismatic for Ln(III) (Figure 15b, c) and the large intermetallic separations ($\sim$9.0 Å) preclude significant electronic interactions between the metals. According to the stronger dative bonds involved for d-block complexes compared to f-block, these helicates have been termed non-covalent lanthanide podates. In the latter complexes, the facial octahedral non-covalent d-block tripod acts as a stable helical non-covalent tripod which organizes the three strands for their coordination to Ln(III) [25]. Optical and magnetic properties can be finely tuned by a judicious choice of metal ions. The use of spectroscopically inert Zn(II) in the non-covalent tripod does not perturb the energy transfer processes occuring at the lanthanide site and (HHH)-$[EuZn(\mathbf{57})_3]^{5+}$ works as an efficient UV $\rightarrow$ vis light-converter in acetonitrile [25]. The recent introduction of a terminal carboxylate group in the new segmental ligand strand **58** provides a self-assembled non-covalent podate (HHH)-$[EuZn(\mathbf{58}\text{-H})_3]^{2+}$ which is stable and strongly emissive in water (Figure 15b), a crucial point if these devices are to find applications as luminescent markers [71]. The introduction of spectroscopically active Fe^{II} in the non-covalent tripod has little effect on the structural and thermodynamic characteristics of the final podate, but it strongly affects the photophysical properties via an efficient intramolecular $Eu^{III} \rightarrow Fe^{II}$ energy transfer process which completely quenches the Eu-centered luminescence in the deep red podates $[EuFe(\mathbf{57})_3]^{5+}$ (Figure 15c) [26]. Compared to the strongly luminescent analogue $[EuZn(\mathbf{57})_3]^{5+}$, the replacement of Zn^{II} by Fe^{II} corresponds to a YES/NO logic gate, a prerequisite for the design of molecular devices performing logic operations if the switching process can be addressed *via* an external signal (electrochemical, optical or magnetic) [72].

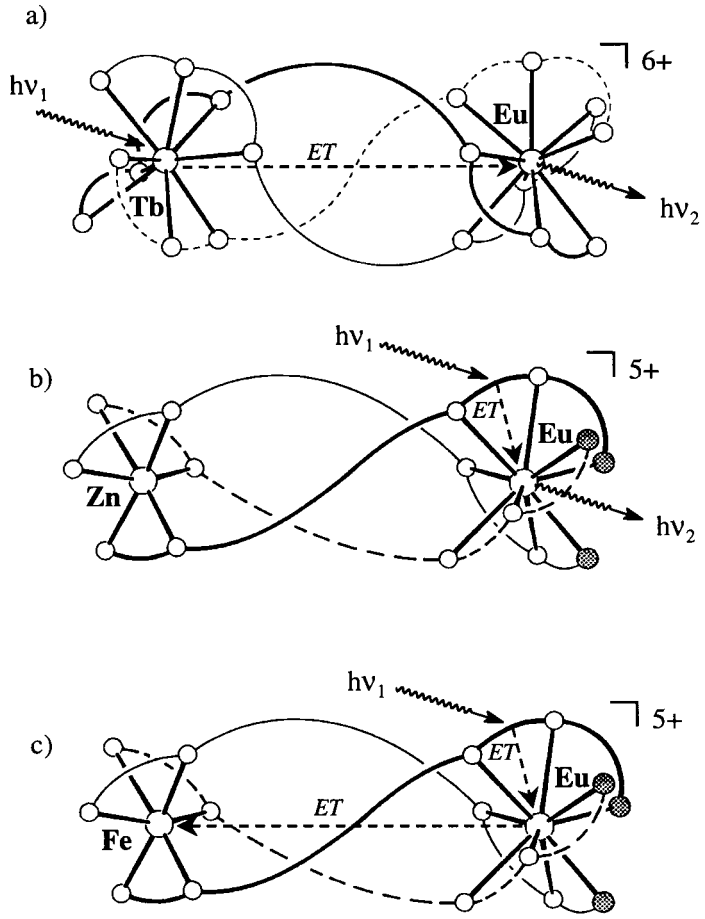

Figure 15. Absorption, energy transfer (ET) and emission processes in self-assembled heterodimetallic helicates: (a) [TbEu(**15**)$_3$]$^{6+}$ as a directional vis $\rightarrow$ vis light converter, (b) [EuZn(**57**)$_3$]$^{5+}$ as a UV $\rightarrow$ vis light converter and (c) [EuFe(**57**)$_3$]$^{5+}$ as a UV light quencher.

The non-covalent podates [LnFe(**57**)$_3$]$^{5+}$ (Ln = La—Lu) also display unusual magnetic properties associated with an isolated Fe(II)-centered thermal spin-crossover ($^1A \rightleftharpoons ^5T$) behaviour [26]. The size of Ln^{III} bound in the nine-coordinate site systematically affects the enthalpic (ΔH_{sc}) and entropic parameters (ΔS_{sc}) of the spin state equilibria (Fe^{II} low spin (diamagnetic) $\rightleftharpoons$ Fe^{II} high spin (paramagnetic)), thus implying a mechanical coupling between the metallic sites via the ligand backbone. A strong thermochromism, resulting from different Fe^{II} ligand-field (d-d) and charge transfer (MLCT) transitions in the two spin states, comes with the magnetic changes leading to fascinating possibilities for the design of thermally and optically addressable magnetic switches [26].

3.3. NEW SYNTHETIC STRATEGIES FOR BUILDING HELICATES

In the perspectives of a recent review dedicated to helicates [2], it was suggested that one might take advantage of kinetically inert helical building blocks to generate polymetallic helicates according to a convergent step-by-step strategy (Figure 16). This approach is particularly attractive for polymetallic helicates because the synthesis of the relevant instructed ligand strands for the recognition of more than two metal ions is often complicated and tedious.

A first step toward this goal has been recently reported by Lam and coworkers who prepared the inert C_3-symmetrical building block FAC-[Ru(**59**)$_3$]$^{2+}$ where three protonated pyrrazole nitrogen atoms point along the threefold axis [74]. Upon reaction with a weak base and Cu(I), FAC-[Ru(**59**)$_3$]$^{2+}$ is deprotonated and selectively produce the dimetallic double-stranded helicate {[Ru(**59**-H)$_3$](Cu)$_3$[Ru(**59**-H)$_3$]}$^{+}$ in which two monometallic triple-helical complexes with the same helicity are put on top of each other and are connected by three linear N(pyr)—Cu(I)—N(pyr) linkers (Figure 17).

Related stepwise assemblies of supramolecular boxes have been observed when the imidazole-containing building blocks [Pd(**60**)Cl]$^{+}$ and [Cu(**60**)Cl$_2$] are deprotonated [74]. A circular tetrameric box [Pd$_4$(**60**-H)$_4$]$^{4+}$ and a hexameric complex [Cu$_6$(**60**-H)$_6$]$^{6+}$ are formed in solution which can be isolated and structurally characterized in the solid state (Figure 18) [74].

The connection of two or more helical building blocks may result from the complexation of bridging ancilliary ligands to unsaturated metal ions. According to this strategy, Constable and coworkers have demonstrated that two head-to-head heterotopic double-stranded helicates (HH)-[Co$_2$(**61**)$_2$(OAc)]$^{3+}$ of opposite helicities assemble to give the bis-bridged centrosymmetrical ('meso') tetrametallic helicate [Co$_2$(**61**)$_2$](μ-OAc)$_2$[Co$_2$(**61**)$_2$]$^{6+}$ in the isolated crystals (Figure 19) [76]. However, the similarity of the ^{1}H-NMR spectrum with previous analogous dimetallic complexes unambigously establish that the acetate bridges do not persist in solution.

4. Summary and Outlook

This brief overview of recent advances in helicate self-assembly highlights the fact that the usual three step approach which has dominated this field during the last decade: (1) synthesis of ligands, (2) isolation of the helicates in the solid state and (3) X-ray crystal structure has reached its limit and considerable interest is now focused on the understanding and control of the thermodynamic equilibria leading to the final organized architecture. When we consider the sizeable structural effects produced by minor changes in the steric, electronic and solvation properties of the components, we realize that a reliable predictive model for helicate self-assembly in polar solvent similar to that developed by Whitesides and coworkers for hydrogen-bonded aggregates in organic solvent [30] will be very difficult to obtain. Nevertheless, the systematic empirical exploration of the subtle factors

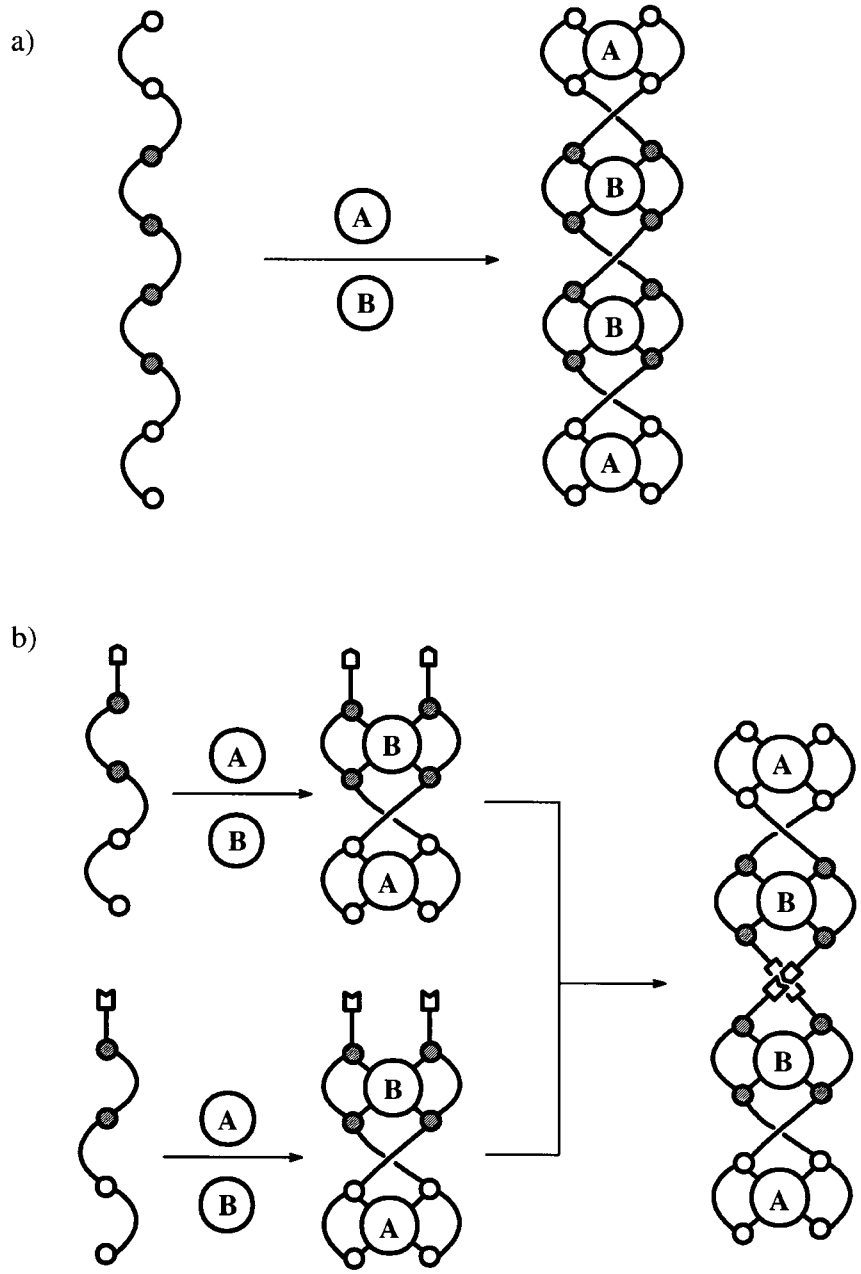

Figure 16. (a) Classical and (b) step-by-step self-assembly of a heterotetrametallic double-stranded helicate. (Reproduced with the permission from Ref [2]. Copyright 1997 American Chemical Society.)

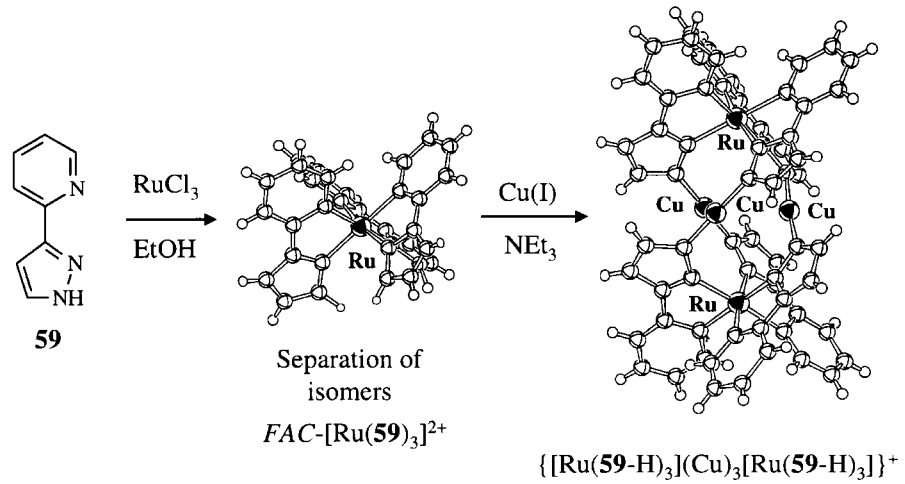

Figure 17. The step-by-step synthesis of the dimetallic triple-stranded helicate $[Ru(\mathbf{59}\text{-}H)_3](Cu)_3[Ru(\mathbf{59}\text{-}H)_3]^{+}$ [73].

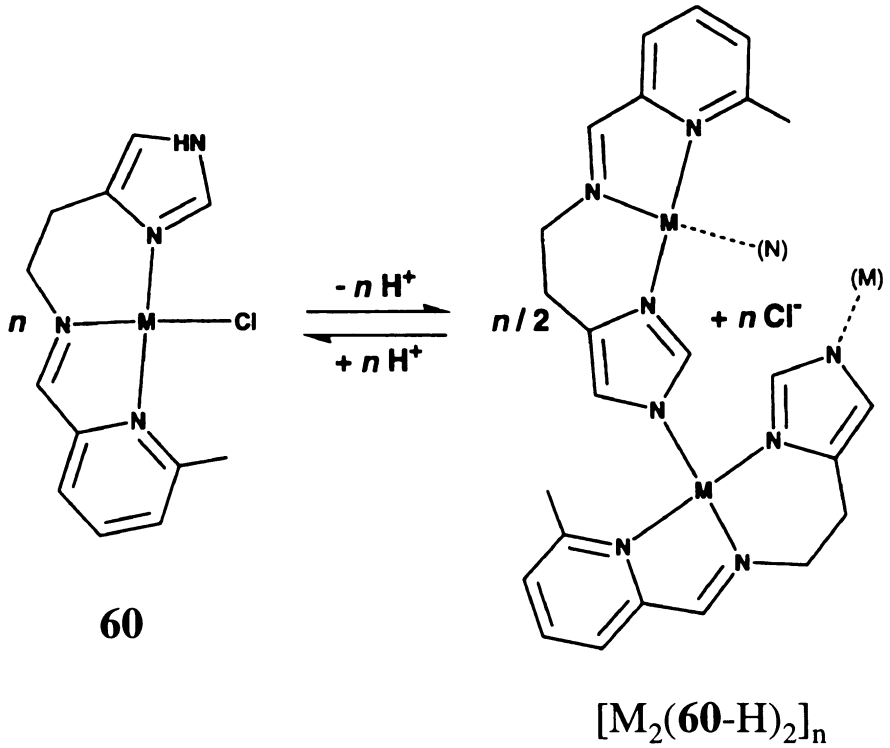

Figure 18. Monomer-oligomer interconversions driven by deprotonation [74]. (Reproduced with the permission from Ref [74]. Copyright 1997 WILEY-VCH Publishers.)

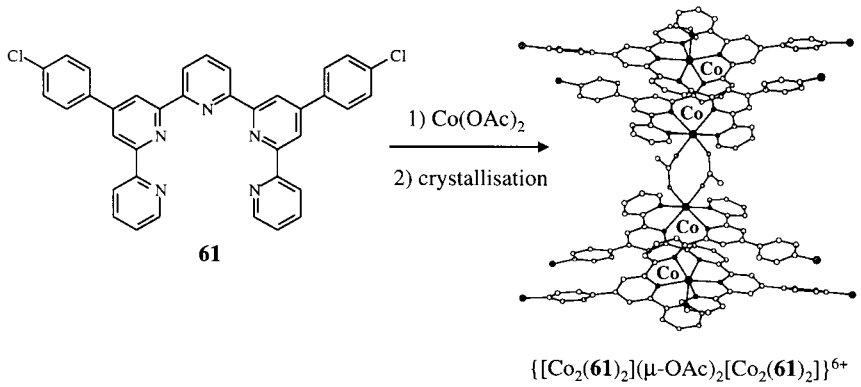

Figure 19. Assembly of the tetrametallic bis-bridged double-stranded helicate $[Co_2(\mathbf{61})_2](\mu\text{-OAc})_2[Co_2(\mathbf{61})_2](PF_6)_6$ in the solid state [75].

controlling the assembly process in solution has led to the discovery and development of one- (catenates) two- (circular helicates) and three-dimensional (cages) structural alternatives to helicates which significantly enlarge the potential applications of these complexes. The high level of structural organization exhibited by these metallosupramolecular complexes, together with their fascinating selective and fast generation under thermodynamic control will find numerous applications in optronic and material sciences. Preliminary applications of heteropolymetallic helicates as self-assembled guests, luminescent probes, magnetic switches and template agents have demonstrated the potentiality of this approach. A significant improvements of the thermal stability, electronic and structural control of the final edifice will open new perspectives for applications of helicates as catalysts [76], sensors [63] and liquid crystals [77].

References

1. J.-M. Lehn, A. Rigault, J. Siegel, J. Harrowfield, B. Chevrier, and D. Moras: *Proc. Natl. Acad. Sci. USA* **84**, 2565 (1987).
2. C. Piguet, G. Bernardinelli, and G. Hopfgartner: *Chem. Rev.* **97**, 2005 (1997).
3. R. S. Cahn, C. Ingold, and V. Prelog: *Angew. Chem. Int. Ed. Engl.* **5**, 385 (1966).
4. J. S. Lindsey: *New J. Chem.* **15**, 153 (1991).
5. A. F. Williams, C. Piguet, and R. Carina: in L. Fabbrizzi and A. Poggi (ed.), *Transition Metals in Supramolecular Chemistry*, p. 404, Kluwer Academic Publishers (1994).
6. E. C. Constable: *Tetrahedron* **48**, 10013 (1992).
7. E.C. Constable: *Prog. Inorg. Chem.* **42**, 67 (1994). E. C. Constable in J. L. Atwood, J. E. D. Davies, D. D. MacNicol, and F. Vögtle (eds.), *Comprehensive Supramolecular Chemistry*, Chap. 6, Pergamon, Oxford (1996).
8. A. F. Williams: *Chem. Eur. J.* **3**, 15 (1997). C. Provent and A. F. Williams in J.-P. Sauvage (ed.), *Transition Metals in Supramolecular Chemistry*, Kluwer Academic Publishers (1998), in press.
9. C. Piguet, G. Bernardinelli, B. Bocquet, A. Quattropani, and A. F. Williams: *J. Am. Chem. Soc.* **114**, 7440 (1992).

10. C. Piguet, G. Hopfgartner, B. Bocquet, O. Schaad, and A. F. Williams: *J. Am. Chem. Soc.* **116**, 9092 (1994).
11. W. Dai, H. Hu, X. Wei, S. Zhu, D. Wang, K. Yu, N. K. Dalley, and X. Kou: *Polyhedron* **16**, 2059 (1997).
12. M. Greenwald, M. Eassa, E. Katz, I. Willner, and Y. Cohen: *J. Electroanal. Chem.* **434**, 77 (1997).
13. R. Ziessel, A. Harriman, J. Suffert, M.-T. Youinou, A. DeCian, and J. Fischer: *Angew. Chem. Int. Ed. Engl.* **36**, 2509 (1997).
14. R. G. Khoury, L. Jaquinod, and K. M. Smith: *Tetrahedron* **54**, 2339 (1998).
15. E. Psillakis, J. C. Jeffery, J. A. McCleverty, and M. D. Ward: *J. Chem. Soc., Chem. Commun.* 479 (1997). E. Psillakis, S. M. Couchman, J. C. Jeffery, J. A. McCleverty, and M. D. Ward: *J. Chem. Soc., Dalton Trans.* 537 (1998).
16. M. J. Hannon, C. L. Painting, A. Jackson, J. Hamblin, and W. Errington: *J. Chem. Soc., Chem. Commun.* 1807 (1997).
17. V. A. Grillo, E. J. Seddon, C. M. Grant, G. Aromi, J. C. Bollinger, K. Folting, and G. Christou: *J. Chem. Soc., Chem. Commun.* 1561 (1997).
18. S. J. Shieh, C. C. Chou, G. H. Lee, C. C. Wang, and S. M. Peng: *Angew. Chem. Int. Ed. Engl.* **36**, 56 (1997).
19. F. A. Cotton, L. M. Daniels, G. T. Jordan, and C. A. Murillo: *J. Am. Chem. Soc.* **119**, 10377 (1997).
20. E. C. Constable, F. Heirtzler, M. Neuburger, and M. Zehnder: *J. Am. Chem. Soc.* **119**, 5606 (1997).
21. M. Albrecht and R. Fröhlich: *J. Am. Chem. Soc.* **119**, 1656 (1997).
22. A. Marquis-Rigault, A. Dupont-Gervais, P. N. W. Baxter, A. Van Dorsselaer, and J.-M. Lehn: *Inorg. Chem.* **35**, 2307 (1996). T. M. Garrett, U. Koert, and J.-M. Lehn: *J. Phys. Org. Chem.* **5**, 529 (1992). A. Pfeil and J.-M. Lehn: *J. Chem. Soc., Chem. Commun*. 838 (1992). R. C. Scarrow, D. L. White, and K. N. Raymond: *J. Am. Chem. Soc.* **107**, 6540 (1985).
23. D. P. Funeriu, J.-M. Lehn, G. Baum, and D. Fenske: *J. Chem. Soc., Chem. Commun.* 1323 (1997). B. Hasenknopf, J.-M. Lehn, B. O. Kneisel, G. Baum, and D. Fenske: *Angew. Chem. Int. Ed. Engl.* **35**, 1838 (1996).
24. R. F. Carina, A. F. Williams, and C. Piguet: *Helv. Chim. Acta* **81**, 548 (1998).
25. N. Martin, J.-C.G. Bünzli, V. McKee, C. Piguet, and G. Hopfgartner: *Inorg. Chem.* **37**, 577 (1998). C. Piguet, J.-C. G. Bünzli, G. Bernardinelli, G. Hopfgartner, and A. F. Williams: *J. Am. Chem. Soc.* **115**, 8197 (1993).
26. C. Piguet, G. Hopfgartner, A. F. Williams, and J.-C. G. Bünzli: *J. Chem. Soc., Chem. Commun.* 491 (1995). C. Piguet, E. Rivara-Minten, G. Hopfgartner, and J.-C. G. Bünzli: *Helv. Chim. Acta* **78**, 1541 (1995). C. Piguet, G. Bernardinelli, J.-C. G. Bünzli, S. Petoud, and G. Hopfgartner: *J. Chem. Soc., Chem. Commun.* 2575 (1995). C. Piguet, J.-C.G. Bünzli, G. Bernardinelli, G. Hopfgartner, S. Petoud, and O. Schaad: *J. Am. Chem. Soc.* **118**, 6681 (1996).
27. C. Piguet, E. Rivara-Minten, G. Hopfgartner, and J.-C. G. Bünzli: *Helv. Chim. Acta* **78**, 1651 (1995). C. Piguet, E. Rivara-Minten, G. Bernardinelli, J.-C. G. Bünzli, and G. Hopfgartner: *J. Chem. Soc., Dalton Trans.* 421 (1997).
28. B. Perlmutter-Hayman: *Acc. Chem. Res.* **19**, 90 (1986).
29. S. Blanc, P. Yakirevitch, E. Leize, M. Meyer, J. Libman, A. vanDorsselaer, A.-M. Albrecht-Gary and A. Shanzer: *J. Am. Chem. Soc.* **199**, 4934 (1997).
30. M. Mammen, E. E. Simanek, and G. M. Whitesides: *J. Am. Chem. Soc.* **118**, 12614 (1996). M. Mammen, E. I. Shakhnovich, J. M. Deutch, and G. M. Whitesides: *J. Org. Chem*. **63**, 3821 (1998).
31. R. Krämer, J.-M. Lehn, and A. Marquis-Rigault: *Proc. Natl. Acad. Sci. USA* **90**, 5394 (1993).
32. D. L. Caulder and K. N. Raymond: *Angew. Chem. Int. Ed. Engl.* **36**, 1440 (1997).
33. D. P. Funeriu, Y.-B. He, H. J. Bister, and J.-M. Lehn: *Bull Soc. Chim. Fr.* **133**, 673 (1996).

34. M. A. Masood, E. J. Enemark, and T. D. P. Stack: *Angew. Chem. Int. Ed. Engl.* **37**, 928 (1998).
35. G. Baum, E. C. Constable, D. Fenske, and T. Kulke: *J. Chem. Soc., Chem. Commun.* 2043 (1997). E. C. Constable, T. Kulke, M. Neuburger, and M. Zehnder: *J. Chem. Soc., Chem. Commun.* 489 (1997). P. Baret, D. Gaude, G. Gellon, and J.-L. Pierre: *New J. Chem.* **21**, 1255 (1997).
36. A. Marquis-Rigault, A. Dupont-Gervais, A. vanDorsselaer, and J.-M. Lehn: *Chem. Eur. J.* **2**, 1395 (1996).
37. M. Meyer, B. Kersting, R. E. Powers, and K. N. Raymond: *Inorg. Chem.* **36**, 5179 (1997). B. Kersting, M. Meyer, R. E. Powers, and K. N. Raymond: *J. Am. Chem. Soc.* **118**, 7221 (1996). B. Kersting, J. R. Telford, M. Meyer, and K. N. Raymond: *J. Am. Chem. Soc.* **118**, 5712 (1996).
38. M. Albrecht and M. Schneider: *J. Chem. Soc., Chem. Commun.* 137 (1998). M. Albrecht and S. Kotila: *Angew. Chem. Int. Ed. Engl.* **35**, 1208 (1996).
39. L. J. Charbonnière, M.-F. Gilet, K. Bernauer, and A. F. Williams: *J. Chem. Soc., Chem. Commun.* **39** (1996). L. J. Charbonnière, A. F. Williams, U. Frey, A. E. Merbach, P. Kamalaprija, and O. Schaad: *J. Am. Chem. Soc.* **119**, 2488 (1997).
40. P. N. W. Baxter, J.-M. Lehn, B. O. Kneisel, and D. Fenske: *Angew. Chem. Int. Ed. Engl.* **36**, 1978 (1997). G. S. Hanan, D. Volkmer, U. S. Schubert, J.-M. Lehn, G. Baum, and D. Fenske: *Angew. Chem. Int. Ed. Engl.* **36**, 1842 (1997). P. N. W. Baxter, J.-M. Lehn, B. O. Kneisel, and D. Fenske: *J. Chem. Soc., Chem. Commun.* 2231 (1997).
41. P. N. W. Baxter, H. Sleiman, J.-M. Lehn, and K. Rissanen: *Angew. Chem. Int. Ed. Engl.* **36**, 1294 (1997). H. Sleiman, P. N. W. Baxter, J.-M. Lehn, K. Airola, and K. Rissanen: *Inorg. Chem.* **36**, 4734 (1997). N. Solladié, J.-C. Chambron, C. O. Dietrich-Buchecker, and J.-P. Sauvage: *Angew. Chem. Int. Ed. Engl.* **35**, 906 (1996).
42. M. Fujita and K. Ogura: *Bull. Chem. Soc. Jpn* **69**, 1471 (1996). M. Fujita and K. Ogura: *Coord. Chem. Rev.* **148**, 249 (1996). M. Fujita, F. Ibukoro, K. Ogura, and K. Yamaguchi: *J. Am. Chem. Soc.* **120**, 611 (1998). P. J. Stang and B. Olenyuk: *Acc. Chem. Res.* **30**, 502 (1997). B. Olenyuk, A. Fechtenkötter, and P. J. Stang: *J. Chem. Soc., Dalton Trans.* 1707 (1998).
43. P. N. W. Baxter, J.-M. Lehn, A. DeCian, and J. Fischer: *Angew. Chem. Int. Ed. Engl.* **32**, 69 (1993).
44. V. L. Pecoraro, A. J. Stemmler, B. R. Gibney, J. L. Bodwin, H. Wang, J. W. Kampf, and A. Barwinski: in K. D. Karlin (ed.), *Prog. Inorg. Chem.* **45**, 83 (1997).
45. C. Piguet, G. Bernardinelli, A. F. Williams, and B. Bocquet: *Angew. Chem. Int. Ed. Engl.* **34**, 582 (1995).
46. D. J. Cardenas and J.-P. Sauvage: *Inorg. Chem.* **36**, 2777 (1997). D. J. Cardenas, P. Gavina, and J.-P. Sauvage: *J. Am. Chem. Soc.* **119**, 2656 (1997).
47. J.-C. Chambron, C. O. Dietrich-Buchecker, J. F. Nierengarten, and J.-P. Sauvage: *J. Chem. Soc., Chem. Commun.* 801 (1993). Z. Huo, C. J. Sunderland, T. N. Nishio, and K. N. Raymond: *J. Am. Chem. Soc.* **118**, 5148 (1996).
48. E. C. Constable and D. Phillips: *J. Chem. Soc., Chem. Commun.* 827 (1997).
49. G. Hopfgartner, C. Piguet, and J. D. Henion: *J. Am. Soc. Mass Spectrom.* **5**, 748 (1994). G. Hopfgartner, C. Piguet, J. D. Henion, and A. F. Williams: *Helv. Chim. Acta* **76**, 1759 (1993).
50. F. M. Romero, R. Ziessel, A. Dupont-Gervais, and A. vanDorsselaer: *J. Chem. Soc., Chem. Commun.* 551 (1996).
51. C. Provent, S. Hewage, G. Brand, G. Bernardinelli, L. J. Charbonnière, and A. F. Williams: *Angew. Chem. Int. Ed. Engl.* **36**, 1287 (1997).
52. O. Mamula, A. von Zelewsky, and G. Bernardinelli: *Angew. Chem. Int. Ed. Engl.* **37**, 290 (1998).
53. P. L. Jones, K. J. Byrom, J. C. Jeffery, J. A. McCleverty, and M. D. Ward: *J. Chem. Soc., Chem. Commun.* 1361 (1997).
54. R. Krämer, J.-M. Lehn, A. DeCian, and J. Fischer: *Angew. Chem. Int. Ed. Engl.* **32**, 704 (1993).

55. B. Hasenknopf, J.-M. Lehn, B. O. Kneisel, G. Baum, and D. Fenske: *Angew. Chem. Int. Ed. Engl.* **35**, 1838 (1996).
56. B. Hasenknopf, J.-M. Lehn, N. Boumediene, A. Dupont-Gervais, A. vanDorsselaer, B. O. Kneisel, and D. Fenske: *J. Am. Chem. Soc.* **119**, 10,956 (1997). B. Hasenknopf and J.-M. Lehn: *Poster 170b: Sequential Self-Assembly of Helicates*. 33rd International Conf. Coord. Chem., Florence (1998).
57. T. Beissel, R. E. Powers, and K. N. Raymond: *Angew. Chem. Int. Ed. Engl.* **35**, 1084 (1996). D. L. Caulder, R. E. Powers, T. N. Parac, and K. N. Raymond: *Angew. Chem. Int. Ed. Engl.* **37**, 1840 (1998).
58. R. W. Saalfrank, A. Stark, K. Peters, and H. G. von Schnering: *Angew. Chem. Int. Ed. Engl.* **27**, 851 (1988). R. W. Saalfrank, B. Hörner, D. Stalke, and J. Stalbeck: *Angew. Chem. Int. Ed. Engl.* **32**, 1179 (1993).
59. R. W. Saalfrank, R. Burak, A. Breit, D. Stalke, R. Herbst-Ilmen, J. Daub, M. Porsch, E. Bill, M. Müther, and A. X. Trautwein: *Angew. Chem. Int. Ed. Engl.* **33**, 1621 (1994).
60. J. S. Fleming, K. L. V. Mann, C. A. Carraz, E. Psillakis, J. C. Jeffery, J. A. McCleverty, and M. D. Ward: *Angew. Chem. Int. Ed. Engl.* **37**, 1279 (1998).
61. E. J. Enemark and T. D. P. Stack: *Angew. Chem. Int. Ed. Engl.* **37**, 932 (1998).
62. E. J. Enemark and T. D. P. Stack: *Inorg. Chem.* **35**, 2719 (1996).
63. B. Linton and A. D. Hamilton: *Chem. Rev.* **97**, 1669 (1997).
64. C. Piguet and J.-C. G. Bünzli: *Chimia* **52**, 579 (1998).
65. M. Meyer, A.-M. Albrecht-Gary, C. O. Dietrich-Buchecker, and J.-P. Sauvage: *J. Am. Chem. Soc.* **119**, 4599 (1997). D. B. Amabilino and J. F. Stoddart: *Chem. Rev.* **95**, 2725 (1995).
66. S. Rigault, C. Piguet, G. Bernardinelli, and G. Hopfgartner: *Angew. Chem. Int. Ed. Engl.* **37**, 169 (1998).
67. M. A. Albrecht and S. Kotila: *Angew. Chem. Int. Ed. Engl.* **34**, 2134 (1995). M. A. Albrecht and S. Kotila: *Angew. Chem. Int. Ed. Engl.* **35**, 1208 (1996). M. A. Albrecht, H. Röttele, and P. Burger: *Chem. Eur. J.* **2**, 1264 (1996). M. Albrecht: *Chem. Eur. J.* **3**, 2058 (1997).
68. R. W. Saalfrank, A. Dresel, V. Seitz, S. Trummer, F. Hampel, M. Teichert, D. Stalke, C. Stalder, J. Daub, V. Schünemann, and A. X. Trautwein: *Chem. Eur. J.* **3**, 2058 (1997).
69. M. A. Houghton, A. Bilyk, M. M. Harding, P. Turner, and T. Hambley: *J. Chem. Soc., Dalton Trans.* 2725 (1997).
70. A. C. Try, M. M. Harding, D. G. Hamilton, and J. K. M. Sanders: *J. Chem. Soc., Chem. Commun.* 723 (1998).
71. S. L. Larson, S. M. Hendrikson, S. Ferrere, D. L. Derr, and C. M. Elliott: *J. Am. Chem. Soc.* **117**, 5881 (1995).
72. C. Edder, C. Piguet, J.-C. G. Bünzli, and G. Hopfgartner: *J. Chem. Soc., Dalton Trans.* 4657 (1997).
73. A. P. de Silva, H. Q. N. Gunaratne, and C. P. McCoy: *Nature* **364**, 42 (1993). P. Ghosh, P. K. Bharadwaj: J. Roy, and S. Ghosh: *J. Am. Chem. Soc.* **119**, 11903 (1997).
74. M. H. W. Lam, S. T. C. Cheung, K.-M. Fung, and W.-T. Wong: *Inorg. Chem.* **36**, 4618 (1997).
75. N. Matsumoto, Y. Mizuguchi, G. Mago, S. Eguchi, H. Miyasaka, T. Nakashimo, and J.-P. Tuchages: *Angew. Chem. Int. Ed. Engl.* **36**, 1860 (1997). M. Mimura, T. Matsuo, T. Nakashima, and N. Matsumoto: *Inorg. Chem.* **37**, 3553 (1998).
76. E. C. Constable, M. Neuburger, L. A. Whall, and M. Zehnder: *New J. Chem.* **22**, 219 (1998).
77. G. Hochwimmer, O. Nuyken, and U. S. Schubert: *Macromol. Rapid Commun.* **19**, 309 (1998).
78. H. Nozary, C. Piguet, P. Tissot, G. Bernardinelli, R. Deschenaux, and M.-T. Vilches: *J. Chem. Soc., Chem. Commun.* 2101 (1997).